Heteroduplex DNA and Meiotic Recombination in *Drosophila*

Sarah J. Radford

A dissertation submitted to the faculty of the University of North Carolina at Chapel Hill in partial fulfillment of the requirements for the degree of Doctor of Philosophy in the Curriculum in Genetics and Molecular Biology.

Chapel Hill
2006

Approved by:

Jeff Sekelsky

Marila Cordeiro-Stone

Robert Duronio

Thomas Petes

Dale Ramsden

ABSTRACT

Sarah J. Radford: Heteroduplex DNA and Meiotic Recombination in *Drosophila*
(Under the direction of Jeff Sekelsky)

Meiotic recombination gives rise to crossovers, which are required in most organisms for the faithful segregation of homologous chromosomes during meiotic cell division. Investigation of the details of this process has centered largely on studies in fungi; however, recent evidence suggests that a complete understanding will require this question to be approached in multiple model organisms.

In this thesis, I report the development of tools for expanding the study of meiotic recombination in *Drosophila melanogaster*. I have combined an existing assay for the selection of rare recombination events with molecular techniques to allow the fine dissection of the structures of recombination events. I demonstrate the utility of this assay by using it to investigate recombination in a known meiotic mutant, *mei-9*. The results of this investigation provide evidence supporting a role for MEI-9 in resolving recombination intermediates to generate crossovers, and supporting a model in which noncrossovers are generated by multiple pathways. I also report the genetic characterization of the role of a partner protein of MEI-9, ERCC1. These results suggest that the functional protein complex for the generation of meiotic crossovers contains MEI-9, ERCC1, and a previously-characterized protein, MUS312.

Additionally, I created a *Drosophila* mismatch repair mutant, *Msh6*, and used my newly-developed assay to investigate meiotic recombination events in this mutant. This constitutes the first investigation of meiotic mismatch repair in *Drosophila*. Results of this assay show that elimination of mismatch repair allows the recovery of unrepaired heteroduplex DNA with high efficiency. Characterization of the structure and arrangement of heteroduplex DNA is instrumental in the dissection of molecular models of meiotic recombination. The creation of a mutant in which heteroduplex DNA can be recovered in *Drosophila* does much to put the molecular characterization of meiotic recombination in this organism on a par with studies in fungi. Using this assay, I also show strong evidence for a "short-patch" repair pathway that acts in the absence of canonical mismatch repair in *Drosophila*.

In this thesis, I demonstrate the importance and effectiveness of using *Drosophila* to further our understanding of the crucial process of meiotic recombination, and report the development of a number of tools that demonstrate the attractiveness of using this model organism for these studies.

ACKNOWLEDGEMENTS

This thesis is the culmination of ideas thought by many people and experiments performed by many hands. I would like to thank all members of the Sekelsky lab, past and present, for their generosity with time, comments and criticisms, and friendship. I would also like to thank my advisor, Jeff Sekelsky, for so many things: the SURE experience that convinced me to go to graduate school, the chance to work on an incredible project, and countless hours of discussion both scientific and otherwise, to name a few.

I would also like to thank a number of people for their specific contributions to this work. Elizabeth Goley made the initial targeted *Ercc1* mutant with accompanying deletion, which I used as a starting point for experiments described in Chapter 2. Kimberly Baxter and Susan McMahan helped with the collection of sensitivity and recombination data also described in this chapter. Hutton Kearney initially characterized the *rosy* alleles which I used for experiments in Chapters 3 and 4. Hutton also began the *mei-9* project, and I would like to thank her for giving me the opportunity to take it on when she left the lab. Mathilde Sabourin generated and molecularly characterized the *Msh6* alleles described in Chapter 4. Last, but certainly not least, the help of Hunter Blanton, Cassie Bowen, Meaghan Martin, Susan McMahan, Sushmita Mukherjee, Mathilde Sabourin, Jeff Sekelsky, and Preston

Sloop was essential for the management of the large-scale recombination experiments described in Chapters 3 and 4.

Finally, I would like to acknowledge the support of several people. Thanks go to Susan McMahan for riding the roller coaster of *rosy* recombination experiments with me: all the way from the lowest valleys to the highest peaks. I would also like to specially thank Lisa Antoszewski, Jan LaRocque, and Susan McMahan for listening to all my tirades and sharing theirs with me. Finally, I would like to thank my family and "family" for their encouragement from the very beginning, and Brian Eggert for being there every single day.

TABLE OF CONTENTS

LIST OF TABLES

Table

LIST OF FIGURES

Figure

LIST OF ABBREVIATIONS

CO: crossover

DHJ: double Holliday junction

DSBR: double-strand break repair

GC: gene conversion

hDNA: heteroduplex DNA

HJ: Holliday junction

MMR: mismatch repair

NCO: noncrossover

NER: nucleotide excision repair

PMS: post-meiotic segregation

SDSA: synthesis-dependent strand annealing

CHAPTER 1

INTRODUCTION

One of the most important parts of the life cycle of any cell is cell division. Cell division leads to the production of a new generation of cells, allowing the propagation of the species in the case of single-celled organisms or the growth and differentiation of multicellular organisms. A special type of cell division called meiosis is required for the production of gametes during sexual reproduction. This process is characterized by two rounds of division: the first is reductional and the second is equational. Reductional division requires the pairing of homologous chromosomes and the generation of crossovers (COs) between paired homologs for the proper segregation of chromosomes.

Meiotic COs are generated by recombination. Several models have been proposed to describe the molecular mechanism of meiotic recombination; however, these models must describe not only the formation of COs, but also the formation of noncrossovers (NCOs) and the association of gene conversion (GC) with both COs and NCOs. GC is a non-reciprocal transfer of information from one chromatid to another, giving rise to a 3:1 or 1:3 segregation of alleles rather than 2:2 Mendelian segregation.

Over forty years ago, Robin Holliday first proposed a model that incorporated all of these observations (HOLLIDAY 1964). In Holliday's model, the initiating lesion is a single-strand nick on both of the chromatids involved and recombination proceeds through a series of structures, culminating in an intermediate that contains a single four-way DNA junction. These junctions have since been named Holliday junctions (HJs) as their existence was first proposed in this model. Holliday's model also proposed that GC is the consequence of the formation and repair of heteroduplex DNA (hDNA), DNA in which each strand of the duplex is derived from a different parental chromosome.

Holliday's model proposed the formation of symmetric hDNA, in which hDNA is formed at the same place on both chromatids. This makes the prediction that failure to repair both tracts of hDNA should give rise to unrepaired hDNA at the same locus on both chromatids. In fact, in many types of fungi, this type of event is not observed at the expected frequencies; rather, results suggested that hDNA might form asymmetrically. To account for this observation, another model was proposed by Meselson and Radding (1975) in which both symmetric and asymmetric hDNA may form. In this model, the initiating lesion is a single-strand nick on only one chromatid, and, like Holliday's model, the key intermediate contains a single HJ.

Evidence from studies of plasmid gap repair in fungi caused the development of a further model (SZOSTAK *et al.* 1983) in which the initiating lesion is a double-strand break (DSB). Like the Meselson and Radding model, this model incorporates both asymmetric and symmetric hDNA. Unlike earlier models, however, the key

intermediate in the DSB repair (DSBR) model contains two HJs. A modified form of the DSBR model (Figure 3.1) is currently the widely-accepted model for meiotic recombination because many of the proposed structures have been detected using physical assays at meiotic recombination hotspots in fungi, including DSBs, strand invasion intermediates, and double-Holliday junction (DHJ) structures (ALLERS and LICHTEN 2001b; CERVANTES *et al.* 2000; COLLINS and NEWLON 1994; SCHWACHA and KLECKNER 1994; SCHWACHA and KLECKNER 1995).

Holliday's model, Meselson's and Radding's model, and the DSBR model are based mostly on observations from studies in fungi. These organisms are particularly amenable to studies of meiotic recombination, and the results of these studies have contributed much to our understanding of this process. Homologs of many of the proteins required for meiotic recombination in fungi are found in other organisms, suggesting that this is a conserved process. Because of this, details about meiotic recombination based on results from fungal studies are often taken as a general rule to be applied to all organisms. Recent evidence has shown, however, that the proteins required in the later stages of CO formation in two types of fungi, *Saccharomyces cerevisiae* and *Schizosaccharomyces pombe*, differ (reviewed in WHITBY 2005). Variation in recombination processes even between species of fungi suggests that this process may encompass more diversity than was previously thought. In fact, it is known that in *Drosophila melanogaster*, a different set of proteins from either of these fungal species is required for the late stages of CO formation (BAKER and CARPENTER 1972; SEKELSKY *et al.* 1995). From these results, it

is clear that a complete understanding of meiotic recombination requires studies in multiple organisms.

Historically, studies of meiotic recombination in *Drosophila melanogaster* have played an important role in our understanding of genetics. For instance, in 1913, Alfred Sturtevant generated the first genetic map using meiotic CO data from *Drosophila* (STURTEVANT 1913), and the utility of genetic screens was first demonstrated looking for *Drosophila* meiotic mutants (BAKER and CARPENTER 1972; SANDLER *et al.* 1968). In addition to a long history of research on *Drosophila* meiotic recombination, there are several features of meiotic recombination in *Drosophila* that make this organism uniquely situated to explore some of the outstanding questions in the field.

As mentioned above, Holliday's model first proposed that COs are the result of nicking HJs, and this proposal has been upheld in more recent molecular models; however, although more than forty years have elapsed since this proposal, researchers have been unable to identify proteins that are required during meiotic recombination to nick HJs. Ten years ago, the *Drosophila* meiotic mutant *mei-9* was cloned, and it was determined that this gene encodes the *Drosophila* homolog of mammalian XPF and *Saccharomyces cerevisiae* Rad1 (SEKELSKY *et al.* 1995), known DNA structure-specific endonucleases (BARDWELL *et al.* 1994; PARK *et al.* 1995). This result, combined with a genetic requirement for *mei-9* late in meiotic recombination (BAKER and CARPENTER 1972; CARPENTER 1982; ROMANS 1980b), makes *Drosophila*

MEI-9 a leading candidate for the long-sought-after nuclear Holliday junction nicking enzyme.

A second proposal of Holliday's is that GC is generated by the formation and repair of hDNA. Later models have upheld this proposal, but the proposed structure and arrangement of hDNA within recombination intermediates differs in these models. In fact, the structure and arrangement of hDNA in the products of meiotic recombination may be used to support or refute different models for the generation of both COs and NCOs. Analysis of hDNA in *S. cerevisiae* meiotic recombination has provided some insight into this process; however, this analysis is limited in detail because detection of hDNA relies on the presence of mismatches. In *S. cerevisiae*, even relatively low numbers of mismatches in a region cause dramatic reductions in meiotic recombination (BORTS and HABER 1987). Levels of heterology ranging from ~0.05% to ~0.3% have been used in experiments in *S. cerevisiae* (BORTS and HABER 1987; GILBERTSON and STAHL 1996; JESSOP *et al.* 2005; JUDD and PETES 1988; MERKER *et al.* 2003; SYMINGTON and PETES 1988); however, the highest levels of heterology have included, at most, three polymorphisms. In *Drosophila*, on the other hand, 0.5% mismatches in a region does not decrease the frequency of recombination (HILLIKER *et al.* 1991). Because of this, analysis of hDNA in *Drosophila* provides an exciting opportunity to obtain a high resolution picture of the hDNA present during meiotic recombination.

In this thesis, I explore both of these interesting facets of meiotic recombination in *Drosophila*. I present evidence that strongly supports the

hypothesis that MEI-9 is indeed a HJ nicking enzyme required for CO formation both through genetic characterization of its known partner, *Ercc1* (Chapter 2), and characterization of meiotic recombination in *mei-9* mutants (Chapter 3). Additionally, I show evidence that supports the double-strand break repair (DSBR) model for meiotic recombination in *Drosophila* through the molecular analysis of recombination events in *mei-9* mutants (Chapter 3) and the creation and analysis of *Msh6* mutants (Chapter 4). Finally, I show evidence that suggests NCOs in *Drosophila* can be generated through several pathways, including synthesis-dependent strand annealing (SDSA) and double Holliday junction (DHJ) dissolution (Chapters 3 and 4). This thesis explores the development of tools useful for the investigation of the process of meiotic recombination in the model organism *Drosophila melanogaster* as well as contributing to our overall understanding of this critical process.

CHAPTER 2

ERCC1 IS REQUIRED FOR A SUBSET OF MEI-9-DEPENDENT MEIOTIC CROSSOVERS[1]

During meiosis, chiasmata form physical linkages between homologous chromosomes that ensure their proper segregation. Chiasmata result from a combination of sister chromatid cohesion and recombinational exchange events called crossovers. Although the molecular mechanism of meiotic crossover formation is not fully known, analysis of recombination events has led to a model with several important features: (1) meiotic recombination initiates with a double-strand break on one chromatid, (2) recombination proceeds through the formation of a heteroduplex-containing intermediate structure with two four-way DNA junctions called Holliday junctions, and (3) crossovers arise through the cleavage of Holliday junctions (STAHL 1996).

In *Drosophila melanogaster*, several genes required for meiotic crossover formation have been identified (MCKIM *et al.* 2002). One such gene is *mei-9*, mutations in which abolish 90% of all meiotic crossovers. Molecular identification of *mei-9* revealed that it encodes the *Drosophila* homolog of Rad1 in *Saccharomyces cerevisiae* and XPF in mammals (SEKELSKY *et al.* 1995). Rad1/XPF is a DNA

[1] This chapter has been published previously (RADFORD *et al.* 2005).

structure-specific endonuclease that is required for nucleotide excision repair (NER), the primary pathway for repair of DNA damage induced by ultraviolet light. NER involves excision of an oligonucleotide containing the damaged bases and fill-in synthesis using the intact strand as a template. Rad1/XPF creates the excision nick 5' to the damaged bases by recognizing a transition in the DNA from 5' double-stranded to 3' single-stranded (BARDWELL *et al.* 1994; PARK *et al.* 1995). Sensitivity of *mei-9* mutants to various DNA damaging agents demonstrates a requirement for MEI-9 in NER as well as other DNA repair pathways (BOYD *et al.* 1976).

Identification of MEI-9 as a protein whose homologs have a DNA-structure-specific endonuclease activity provides a clue to the role MEI-9 may play in meiotic crossover formation. We have previously proposed that MEI-9 acts as a DNA endonuclease on Holliday junctions during meiotic recombination to resolve the intermediate DNA structure into crossover products (SEKELSKY *et al.* 1995). This proposal predicts that the MEI-9 endonuclease is modified during meiotic recombination to change the specificity from that of the NER substrate to that of a Holliday junction.

Rad1/XPF is the catalytic subunit of the NER 5' endonuclease. Rad1/XPF forms a complex with a second protein called Rad10 in *S. cerevisiae* and ERCC1 in mammals. This second, non-catalytic subunit is required for enzymatic activity (DAVIES *et al.* 1995). Mutations in either gene have identical phenotypes in both *S. cerevisiae* (IVANOV and HABER 1995; PRAKASH *et al.* 1985; SCHIESTL and PRAKASH 1990) and mouse (TIAN *et al.* 2004; WEEDA *et al.* 1997). The *Drosophila* homolog of

Rad10/ERCC1 was identified by sequence homology and has been named ERCC1 (SEKELSKY *et al.* 2000b). Additionally, we recently identified a novel protein, MUS312, that physically interacts with MEI-9 to generate crossovers, but that is not required for NER (YILDIZ *et al.* 2002). This leads to the interesting possibility that the substrate specificity of MEI-9 is affected by the partner protein(s) present. Two possible alternatives are: MUS312 may add to the MEI-9-ERCC1 endonuclease complex or MUS312 may replace ERCC1 in the complex to change the substrate specificity. To distinguish between these models, characterization of *Drosophila* ERCC1 is necessary.

We report here the generation of a *Drosophila Ercc1* mutant by homologous targeting. Genetic characterization of this mutant reveals a hypersensitivity to DNA damaging agents that is identical to that of *mei-9*. In contrast, *Ercc1* mutants have a less severe meiotic phenotype than *mei-9* mutants. We find that levels of MEI-9 protein are decreased in *Ercc1* mutants; however, overexpression of MEI-9 protein in an *Ercc1* mutant is not sufficient to restore meiotic crossing over. We conclude that MEI-9 can generate some meiotic crossovers in the absence of ERCC1. This is the first report of an ERCC1/Rad10-independent function for MEI-9/XPF/Rad1.

RESULTS AND DISCUSSION

Vectors for gene targeting in Drosophila: We used the gene targeting method developed by Rong and Golic (2000) to knock out *Ercc1*. In this method, the desired mutation is initially introduced into the genome as a *P* element

transgene. The genomic fragment to be used for targeting is flanked by FLP recombination targets (FRTs), and carries a recognition sequence for the *I-Sce*I endonuclease. We built a pair of vectors to be used in generating such transgenes. p*P*{Target} is derived from p*P*{CaSpeR4} (PIRROTTA 1988) and contains two FRTs flanking an *I-Cre*I site, *mini-white* gene, and multiple cloning site. As described below, we used p*P*{Target} to knock out *Ercc1*. We also built a derivative, p*P*{TargetB}, that is smaller (6377 bp) and has several additional cloning sites (Figure 2.1). We and others have successfully used this vector to target additional genes (MD Adams and JJS, unpublished data, DONALDSON *et al.* 2004). These vectors have been made available at the Drosophila Genomic Resources Center (http://dgrc.cgb.indiana.edu).

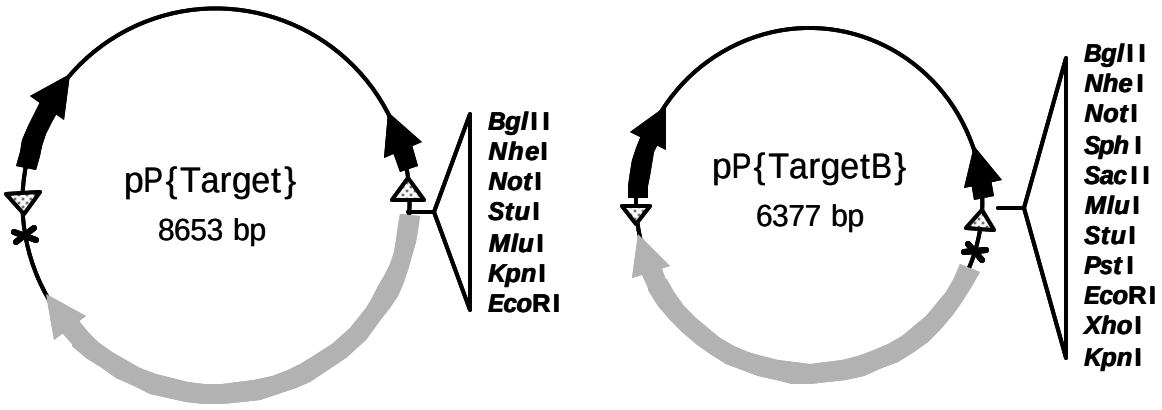

Figure 2.1. Vectors for gene targeting in *Drosophila*. Schematic maps of p*P*{Target} and p*P*{TargetB} are shown. Both vectors carry a *mini-white* marker gene (gray arrow), FLP recombinase target sites (FRTs; hatched triangles), an *I-Cre*I endonuclease recognition sequence (X), and *P* element ends for transposition (black arrows). The two vectors differ in size and in restriction sites available for cloning.

Targeted knockout of Ercc1: We designed an *Ercc1* targeting construct, p*P*{*Ercc1*^{X}}, that carries a 4.7-kb genomic fragment. In addition to *Ercc1*, this fragment includes 1.8 kb of *Smc2*, all of *CG12797*, and the 5' end of *CG12855* (Figure 2.2A). The predicted protein product of *CG12797* consists of seven WD40 repeats, and is 60% identical to human Ciao1 over its entire length of 335 residues. Ciao1 was originally isolated on the basis of its interaction with the Wilms' tumor suppressor WT1 (JOHNSTONE *et al.* 1998). The predicted protein product of *CG12855* consists of 596 residues, with ~200 residues in each of two regions that are 45-55% similar to human HPS. Mutations in HPS are associated with Hermansky-Pudlak syndrome, a recessive autosomal disorder of cytoplasmic organelles (OH *et al.* 1996). We will refer to *CG12797* as *Ciao1* and *CG12855* as *HPS*.

We inserted two base pairs into *Ercc1* to generate a frameshift at codon 96 (out of 259), upstream of the most highly conserved region. The insertion generates an *Xho*I site, which can be used as a diagnostic marker for the mutation. An *I-Sce*I site was inserted 569-bp downstream of the *Xho*I site, within the *Ercc1* 3' untranslated region. We generated two insertions by germline transformation, one on the *X* and the other on chromosome *3*. Additional autosomal insertions were generated by transposing the *X*-linked insertion.

We used the *X*-linked insertion of *P*{*Ercc1*^{X}} and five autosomal insertions to generate putative targeted insertions, as described in Rong and Golic (2001). Of 16 insertions of the targeting DNA, three mapped to chromosome *2*, and one of these was a homologous insertion into the endogenous *Ercc1* locus. In the ends-in

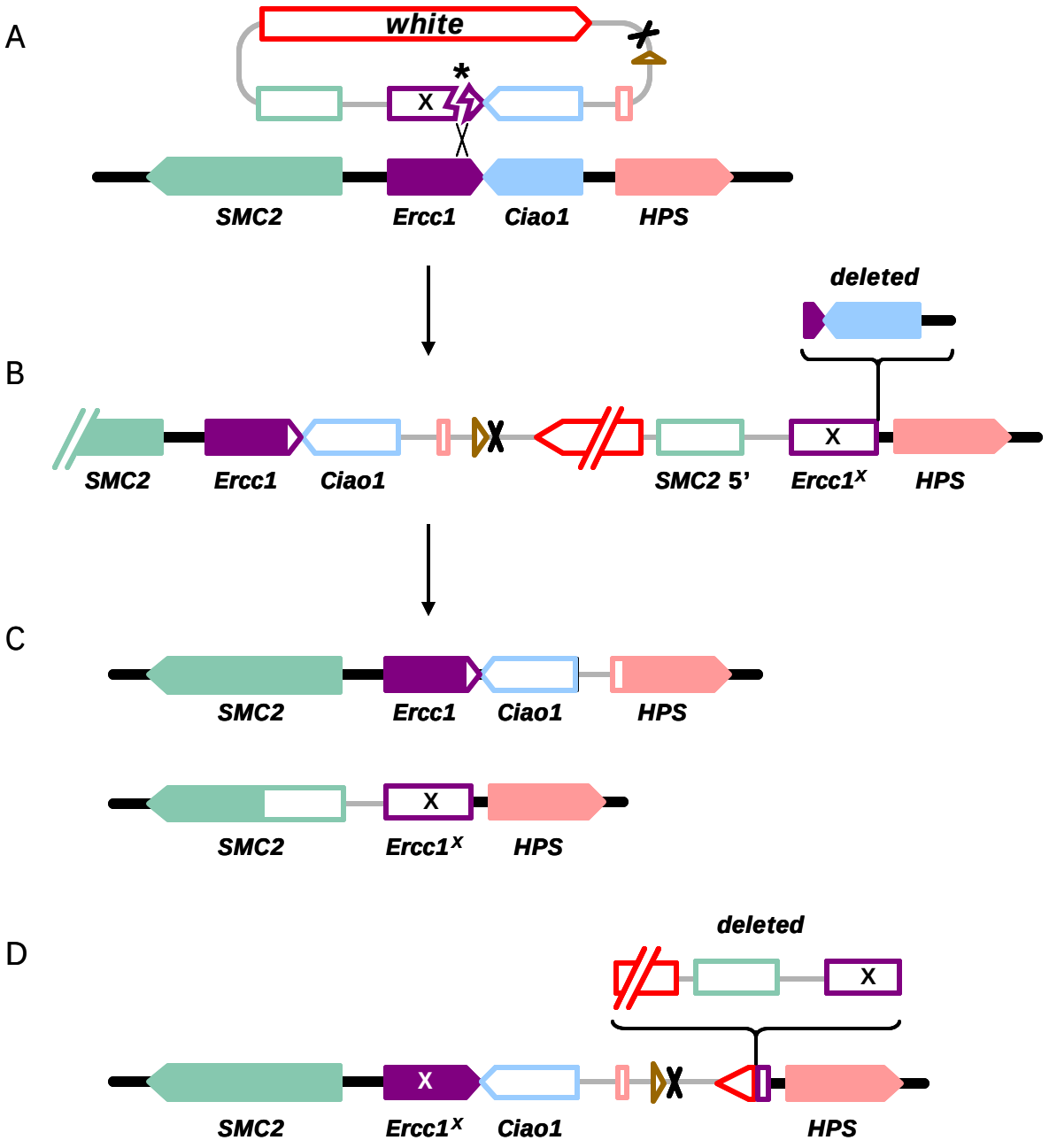

Figure 2.2. Targeting of *Ercc1*. A. Genes from the *Ercc1* genomic region are shown as filled arrows (indicating direction of transcription) on a black line, and genes on the targeting DNA are shown as open arrows or boxes on a gray line. The targeting DNA is shown after excision by FLP recombinase and cutting by *I-Sce*I endonuclease, with an asterisk marking the site of the double-strand break. This targeting fragment is drawn to show alignment of sequences with homology between the targeting DNA and the genomic

DNA. The *Xho*I site introduced into *Ercc1* is indicated by an X. The *mini-white* marker gene and the FRT and *I-Cre*I sites are as in Figure 2.1. B. The predicted product of ends-in integration is shown, with sequences derived from the targeting DNA in open symbols and chromosomal sequences as filled symbols. The region deleted in the integration we recovered is indicated. C. Predicted products from reduction of the tandem duplication after cutting with *I-Cre*I and repair by single-strand annealing. One product is completely wild-type (top), and the other carries $Ercc1^{X}$ and the adjacent deletion of *Ciao1* (bottom). D. The structure of the mutation used in these studies is shown. It is equivalent to the targeted integration depicted in (B), except that most of *mini-white* and one copy of *Ercc1* have been deleted, and the remaining copy of *Ercc1* carries the *Xho*I mutation.

method of gene targeting, the result of integration of targeting DNA into the homologous target is a tandem duplication. Analysis of the targeted integration into *Ercc1* that we recovered revealed that it was imprecise, containing a 1569 bp deletion on one copy of the duplication (Figure 2.2B and Figure 2.3). This deletion begins at the *I-Sce*I cut site and removes the 3' UTR of *Ercc1* and all of *Ciao1*, ending 120 bp upstream of the beginning of the *HPS* protein-coding region.

When a double-strand break is introduced between the two copies of a tandem duplication, repair by single-strand annealing (SSA) results in reduction of the duplication to single copy with high efficiency (IVANOV *et al.* 1996). As described by Rong and Golic (2002), we used the rare-cutting endonuclease *I-Cre*I to generate reductions of our tandem duplication. We initially recovered 21 reductions. Eleven of these carried the wild-type *Ercc1* and did not have the associated deletion; these were homozygous viable. The other ten carried the $Ercc1^{X}$ allele, but also had the adjacent deletion. All ten of these were homozygous and hemizygous lethal. These

two types of events are the predicted products of the SSA model for reduction (Figure 2.2C).

The lethality of the chromosome carrying *Ercc1*^{X} and the adjacent deletion was rescued by crossing in a copy of the *P*{*Ercc1*^{X}} targeting construct. The only functional gene on this construct is *Ciao1*, so we conclude that the lethality is due entirely to the deletion of *Ciao1*.

Although the *Ercc1* mutation and the deletion were 100% linked in the original reductions that we recovered, we thought that we might be able to separate the two by generating a larger number of reductions. We devised a scheme in which putative reductions were recovered in trans to *Df(2R)knSA3*, which deletes the entire region, and we screened the hemizygous viable reductions for the presence of the *Ercc1*^{X} mutation. We recovered one such event after analyzing only four reductions; however, the structure of this reduction was more complex than we had anticipated.

We performed a PCR with forward primers specific to either the wild-type *Ercc1* locus or the *Ercc1*^{X} mutation and a reverse primer within *HPS* just downstream of the sequence included in the original targeting vector. We expected a product of ~2.4 kb in the wild-type genotype with the *Ercc1*-specific primer, a product of ~800 bp in the targeted duplication with the *Ercc1*^{X}-specific primer (as a result of the ~1600 bp deletion), and a product of ~2.4 kb in the *Ercc1*^{X} genotype. We saw the first two expected products; however, instead of an ~2.4 kb product, we saw an ~1.2 kb product with the *Ercc1*^{X}-specific primer in *Ercc1*^{X} (Figure 2.3). Sequencing

of this product led us to conclude that the *Ercc1*^{X}-specific primer had annealed to the weakly complementary sequence surrounding an *Xho*I site downstream of the FRT in the original targeting vector, and that the *I-Cre*I site used to induce collapse of the duplication remains intact in the reduction. Further PCR and sequencing reactions (see Materials and Methods for details) show that no wild-type *Ercc1* is present, only the *Xho*I-interrupted *Ercc1*. There is also one wild-type copy of *Ciao1*; however, there remains 1218 bp of extra sequence from the original targeting vector in the intergenic region between *Ciao1* and *HPS* (Figure 2.2D). The recovered reduction, then, is mutant for *Ercc1* and wild-type for *Ciao1*.

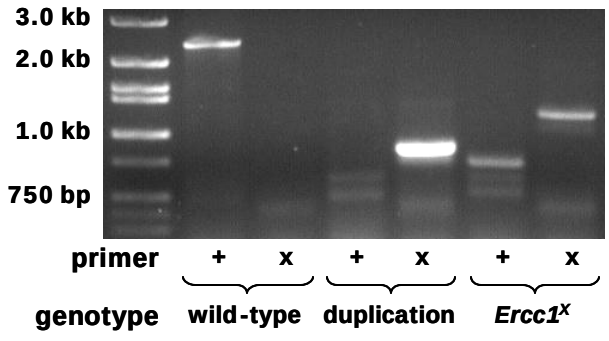

Figure 2.3. Molecular analysis of tandem duplication and *Ercc1*^{X} reduction. Allele-specific PCR was performed using either an *Ercc1*-specific primer (+) or *Ercc1*^{X}–specific primer (X) and a reverse primer complementary to sequence outside of the targeting sequence. PCR reactions were run on a standard agarose gel for analysis. The expected 2.4 kb product is seen with the + primer in wild-type; however, the expected 2.4 kb product is missing with the X primer in *Ercc1*^{X} and instead a 1.2 kb product is seen. A 800 bp product is seen with the X primer in the duplication, confirming the presence of the 1.6 kb deletion.

The insertion of 1218 bp of vector sequence is 120 bp upstream of the *HPS* start of translation. It is possible that this insertion disrupts *HPS* function in the *Ercc1*^{X} reduction allele. We wanted to ensure that any meiotic phenotype seen using the reduction allele could be attributed to the targeted mutation of *Ercc1*, and

not the insertion of DNA upstream of *HPS*. Although we do not have an allele of *HPS* identical to that in the reduction allele in conjunction with wild-type *Ercc1*, we do have an allele of *HPS* that has an insertion of 7480 bp in the same location, and is wild type for *Ercc1*: the original targeted duplication (Figure 2.2B). If the insertion of 1218 bp in the reduction allele is affecting *HPS* expression, it is likely that this larger insertion would mimic or exacerbate the effect. We assayed *X* nondisjunction in females homozygous for the original targeted duplication (see below for an explanation of the *X* nondisjunction assay). We did not see any *X* nondisjunction (n=218), indicating that the insertion upstream of *HPS* likely does not contribute to the meiotic phenotype.

Ercc1 mutants are hypersensitive to UV and MMS: *mei-9* mutants are hypersensitive to several DNA damaging agents, indicating a role for MEI-9 in DNA repair pathways including NER (BOYD *et al.* 1976). To determine what role, if any, *Drosophila* ERCC1 plays in NER, we tested the sensitivity to killing of $Ercc1^{X}$ mutants in response to treatment with ultraviolet light (UV). UV induces primarily pyrimidine dimers and 6-4 photoproducts, both of which are repaired by NER.

$Ercc1^{X}$ mutants are equally as sensitive to UV treatment as *mei-9* mutants, indicating that ERCC1 is indeed important for NER (Figure 2.4). Both $Ercc1^{X}$ homozygous and hemizygous (over *Df(2R)knSA3*, a deficiency for the region) mutants display an equal sensitivity to UV treatments over a variety of doses, indicating that $Ercc1^{X}$ is genetically null in this assay (Figure 2.4). We also see that $Ercc1^{X}$ mutants and *mei-9* mutants are equally as sensitive to treatment with

another type of DNA damaging agent methyl methanesulfonate (MMS) (data not shown).

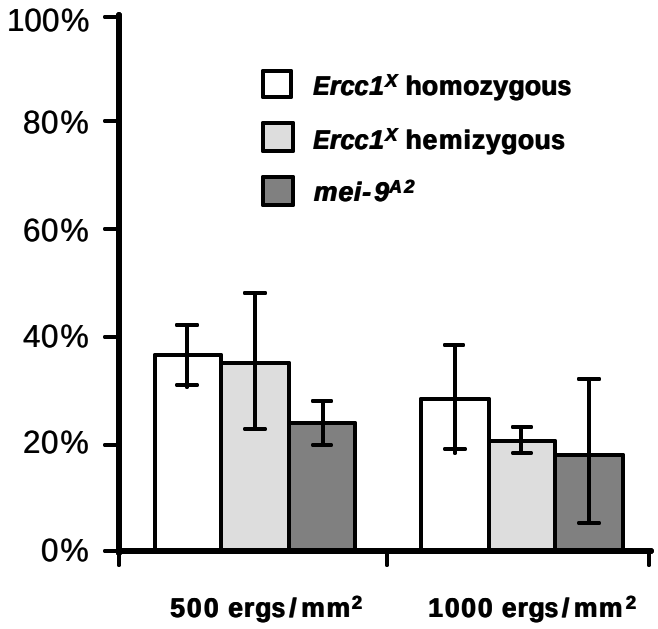

Figure 2.4. Sensitivity to killing by UV light of *Ercc1*^{X} and *mei-9* mutants. Percentage survival, relative to wild-type controls, after exposure of larvae to 500 and 1000 ergs/mm^2 (1 erg/mm^2 = 0.1 J/m^2) of UV light is shown for *Ercc1*^{X} homozygous and hemizygous mutants and *mei-9*^{A2} mutants. Bars indicate standard deviations.

Loss of ERCC1 function confers a meiotic phenotype that is less severe than loss of MEI-9 function: MEI-9 is required to generate most meiotic crossovers. The chiasmata produced by crossovers are essential for proper segregation of homologs during meiosis I; therefore, in the absence of normal levels of crossovers there are high levels of meiosis I chromosome nondisjunction. In *Drosophila*, *X* chromosome nondisjunction can be measured by the use of appropriate genetic markers, giving an indirect assay for recombination defects. Wild-type levels of *X* nondisjunction are ~0.3%, whereas null *mei-9* mutants have ~25-35% *X* nondisjunction (YILDIZ *et al.* 2004). In *Ercc1*^{X} mutants, there is only 16% *X* nondisjunction (Table 2.1). Although this is a 50-fold increase over wild-type, indicating a severe meiotic defect, it is still only half the level of nondisjunction seen in *mei-9* mutants.

TABLE 2.1. *X* chromosome nondisjunction in *Ercc1* mutants

Genotype	Progeny			*X* nondisjunction (%)
	Normal	Nullo-*X*	Diplo-*X*	
Wild type	1473	2	0	0.3
zygotic *mei-9*^{A2} [1]	857	111	145	37
zygotic *Ercc1*^{X}	1848	91	82	16
zygotic *Ercc1*^{X}*/Df*	1223	23	37	9
m/z *Ercc1*^{X}	1049	55	103	23
P{*WUF9*}, m/z *Ercc1*^{X}	775	80	60	27

[1] The *mei-9* data are from (YILDIZ *et al.* 2004).

To assess more directly the recombination defect in *Ercc1*^{X} mutants, we measured crossing over along the 3rd chromosome. We examined three intervals from *Ly*, in the middle of the left arm, to *e*, in the middle of the right arm (Table 2.2). The total map distance was 35.0 map units in wild-type, but only 8.5 map units in *Ercc1*^{X} mutants, a reduction of 76%; however, map distance was 5.1 map units in *mei-9*^{A2} mutants, a reduction of 85% from the wild-type level. As seen in the *X* nondisjunction assay, *Ercc1* mutants have a less severe defect in crossing over than *mei-9* mutants.

One possible explanation for the less severe meiotic phenotype of the *Ercc1*^{X} mutant is that maternal ERCC1 protein deposited during oogenesis may perdure and partially compensate for the lack of ERCC1 protein produced in an *Ercc1*^{X} mutant. To test this possibility, we measured *X* nondisjunction in *Ercc1*^{X} mutants derived

TABLE 2.2 Meiotic crossing over in *Ercc1* and *mei-9* mutants

Genotype	Exchange within the interval (map units)			Total map distance (map units)	% of wild-type	n
	Ly-st	*st-ry*	*ry-e*			
Wild type	4.1	9.2	21.7	35.0	100%	1887
zygotic *Ercc1*^{X}	0.9	1.6	6.0	8.5	24%	3464
m/z *Ercc1*^{X}	0.6	1.3	2.8	4.7	13%	2007
zygotic *Ercc1*^{X}*/Df*	1.4	2.8	8.5	12.8	37%	4226
m/z *Ercc1*^{X}*/Df*	0.8	2.1	2.5	5.5	16%	1063
zygotic *mei-9*^{A2}	0.4	0.8	3.9	5.1	15%	1862
m/z *mei-9*^{A2}	0.3	1.1	1.3	2.7	8%	2006

from *Ercc1*^{X} mutant mothers. These maternal/zygotic (m/z) *Ercc1*^{X} mutants have higher levels of *X* nondisjunction than zygotic *Ercc1*^{X} mutants (Table 2.1), similar to the levels seen in *mus312* mutants and some *mei-9* alleles (YILDIZ *et al.* 2004; YILDIZ *et al.* 2002). Direct measurements of crossing over also show that m/z *Ercc1*^{X} mutants have a reduction in crossovers similar to zygotic *mei-9* mutants; however, we also find that m/z *mei-9* mutants have a stronger overall reduction in crossing over than either m/z *Ercc1*^{X} or zygotic *mei-9* mutants (Table 2.2). This indicates that there may be a maternal effect in *mei-9* mutants as well as *Ercc1* mutants. We conclude that a maternal effect is not masking the true *Ercc1*^{X} phenotype, but rather that the *Ercc1*^{X} mutant truly causes a less severe reduction in crossovers than a *mei-9* mutant. These results also show that the residual crossovers in *mei-9*

mutants are not due to perdurance of maternal protein, but rather to a secondary, MEI-9-independent pathway.

A second possible explanation for the less severe meiotic phenotype of *Ercc1*^{X} mutants is that this allele is not null for meiotic function. Although this allele creates a frameshift approximately halfway through the coding region of *Ercc1*, there may be some read-through that produces residual functional protein. If this were the case, then reducing the copy number of *Ercc1*^{X} would result in a more severe meiotic phenotype; however, we find that this is not the case. *X* nondisjunction of *Ercc1*^{X} hemizygotes is lower than that of *Ercc1*^{X} homozygotes (Table 2.1, 9% vs. 16%). This evidence also argues against the possibility that the genetic background of the *Ercc1*^{X} mutant is responsible for the less severe meiotic phenotype. The hemizygous case should dilute the background effects, resulting in a more severe meiotic phenotype than the homozygous, but the opposite is true.

The finding that a homozygous *Ercc1*^{X} mutant has a more severe phenotype than a hemizygous *Ercc1*^{X} mutant raises the concern that the *Ercc1*^{X} allele encodes a protein that is acting as a gain-of-function antimorph. To test whether *Ercc1*^{X} encodes a dominant antimorph, we assayed *X* nondisjunction in the following genotypes: (1) one copy of *Ercc1*^{X} and one copy of wild-type *Ercc1*, (2) one copy of a deficiency chromosome that removes *Ercc1* and one copy of wild-type *Ercc1*, (3) two copies of *Ercc1*^{X} and one copy of wild-type *Ercc1*. If *Ercc1*^{X} were acting as a dominant gain-of-function antimorph, we would expect to see wild-type levels of *X* nondisjunction in (2) and increased nondisjunction in (1) and (3); however, we saw

wild-type levels in all three genotypes (data not shown). This shows that *Ercc1*^{X} does not encode a dominant antimorphic form of ERCC1.

Although the *Ercc1*^{X} allele is not acting as a dominant antimorph, there remained the concern that the less severe meiotic defect of this allele is the result of a recessive gain-of-function antimorphic protein rather than a loss of ERCC1 function. There are two possibilities: the *Ercc1*^{X} protein antagonizes (1) the wild-type ERCC1 protein or (2) some other protein. To address these possibilities, we assayed *X* nondisjunction and meiotic recombination in zygotic and m/z hemizygous *Ercc1*^{X} mutants. Because only zygotic mutants retain some ERCC1 protein, the first possibility predicts that the zygotic homozygous *Ercc1*^{X} mutant would have a more severe meiotic defect than the zygotic hemizygous mutant (2 doses of *Ercc1*^{X} vs. 1 dose, equal doses of maternal ERCC1), while the two m/z mutants would have similar phenotypes (no ERCC1 to be antagonized.) On the other hand, the second possibility predicts that the more ERCC1^{X} protein present, the more severe we would expect the phenotype to be (i.e., m/z *Ercc1*^{X} is more severe than zygotic *Ercc1*^{X} which is more severe than m/z hemizygous which is more severe than zygotic hemizygous.) Our results are consistent with the first possibility - that *Ercc1*^{X} may encode an antimorphic protein that antagonizes the maternal ERCC1 protein (Table 2.2). An alternative interpretation of our results is that *Ercc1*^{X} is a loss-of-function mutation and the difference in severity between the zygotic homozygous mutant and the zygotic hemizygous mutant reflects a background effect on the stability of maternally-deposited ERCC1 protein.

Whether *Ercc1*^{X} encodes a protein that antagonizes maternally-deposited ERCC1 protein or whether the varying degrees of phenotype severity reflect a background effect, these results suggest that the m/z *Ercc1*^{X} homozygous and hemizygous mutants represent the complete loss of ERCC1 function. The complete loss of ERCC1 function therefore confers a less severe meiotic defect than the complete loss of MEI-9 function (Table 2.2).

MEI-9 protein is unstable in the absence of ERCC1: In mammalian XPF- or ERCC1-deficient cells, the respective partner protein is generally undetectable by western blot, indicating that complex formation between these two proteins may be important for stability (HOUTSMULLER *et al.* 1999). We performed western blots on whole ovary extracts from *Ercc1*^{X} mutants and probed with an anti-MEI-9 polyclonal antibody. We find that MEI-9 protein is severely decreased, though still detectable, in m/z *Ercc1*^{X} mutants (Figure 2.5). Knowing that complex formation with ERCC1 is important for the stability of MEI-9, we also investigated whether complex formation with MUS312 affects MEI-9 protein levels, because MUS312 must physically interact with MEI-9 to generate meiotic crossovers (YILDIZ *et al.* 2002). The absence of MUS312 had no detectable effect on MEI-9 protein levels (data not shown).

It is possible that the meiotic defect in *Ercc1*^{X} mutants is actually due to the decreased level of MEI-9, and not to absence of ERCC1 per se. To test genetically whether low MEI-9 protein is responsible for the *Ercc1*^{X} meiotic defect, we created a transgene, *P*{WUF9}, encoding FLAG-tagged MEI-9 under the control of the

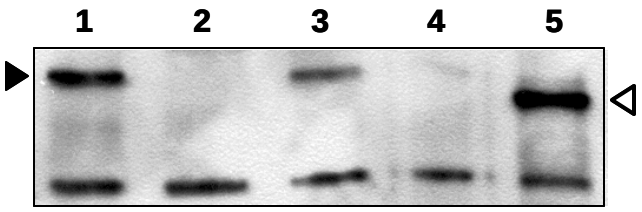

Figure 2.5. Expression of MEI-9 in ovaries. Ovarian proteins were separated on a polyacrylamide gel, transferred to PVDF membrane, and detected with polyclonal anti-MEI-9 serum. Genotypes of ovaries are (1) wild-type, (2) *mei-9*^{A2}, (3) zygotic *Ercc1*^{X}, (4) maternal/zygotic *Ercc1*^{X}, (5) *P*{*WUF9*} in mater-nal/zygotic *Ercc1*^{X}. MEI-9 is indicated by an arrowhead (M_r = 125 kDa). The antiserum also detects unknown proteins of lower molecular weight; one of these is included as a loading control. FLAG-tagged MEI-9 protein (open arrowhead) produced from the *P*{*WUF9*} transgene migrates slightly faster than untagged MEI-9 (M_r = 113 kDa). The *mei-9* cDNA used to make this construct lacks 35 nonessential amino acids at the N terminus (see Materials and Methods for details.)

Ubiquitin promoter. Insertions of *P*{WUF9} fully rescue *mei-9* mutant phenotypes, including sensitivity to MMS and X chromosome nondisjunction (data not shown).

We crossed an insertion of *P*{WUF9} on the *X* chromosome into the *Ercc1*^{X} background to determine whether overexpressing MEI-9 protein can rescue the *Ercc1*^{X} meiotic defect. This transgene does provide an increased level of MEI-9 protein in ovaries (Figure 2.5); however, it has no effect on *X* chromosome nondisjunction levels of *Ercc1*^{X} mutants (Table 2.1). These results suggest that the meiotic defect in *Ercc1*^{X} mutants is likely due to a lack of ERCC1 protein rather than low levels of MEI-9. One caveat to this experiment is that meiotic cells in pachytene (where recombination is occurring) make up a small percentage of the *Drosophila* ovary. It is possible that the increased MEI-9 protein in *Ercc1*^{X} ovaries containing *P*{WUF9} is limited to the non-meiotic cells of the ovary. This could explain the

failure to rescue the *Ercc1*^{X} meiotic defect; however, *P*{WUF9} is able to fully rescue the meiotic defects of *mei-9* mutants (data not shown), indicating that this construct is able to express functional MEI-9 in pachytene.

It is not surprising that the decreased level of MEI-9 protein in *Ercc1*^{X} mutants may not be the cause of the meiotic defect. MEI-9 protein is undetectable by western blot in the ovaries of *mei-9*^{RT1} mutants, but these mutants have a very weak meiotic defect (2% *X* nondisjunction) (YILDIZ *et al.* 2004), suggesting that very little MEI-9 protein may be necessary for generating meiotic crossovers. Once again, the caveat of this experiment is that the majority of ovary tissue is not undergoing meiotic recombination. MEI-9 protein may be decreased or absent in the majority of the cells of the *mei-9*^{RT1} ovary, but present at near wild-type levels in the pachytene cells, leading to the weak meiotic defect.

Taken together, the fact that little MEI-9 protein seems to be required for almost wild-type levels of meiotic recombination in *mei-9*^{RT1} mutants, and *P*{WUF9} expresses seemingly excess MEI-9 protein in the *Ercc1*^{X} background, but is unable to rescue the meiotic phenotype, suggests that lack of ERCC1 protein is responsible for the lack of meiotic recombination in *Ercc1*^{X} mutants.

MEI-9, MUS312, and ERCC1 physically interact by yeast two-hybrid: Prior to this study, we had proposed two alternative scenarios: (1) MUS312 adds to the MEI-9-ERCC1 heterodimer or (2) MUS312 replaces ERCC1 to change the substrate specificity of MEI-9 from that of the NER substrate to a meiotic recombination intermediate, such as a Holliday junction. Although it has been shown that MEI-9

and ERCC1 (YILDIZ *et al.* 2004) and MEI-9 and MUS312 (YILDIZ *et al.* 2002) physically interact by yeast two-hybrid, and that these interactions map to different regions of MEI-9 (YILDIZ *et al.* 2004), evidence for all three proteins participating in a single complex, as predicted by the first scenario, was lacking.

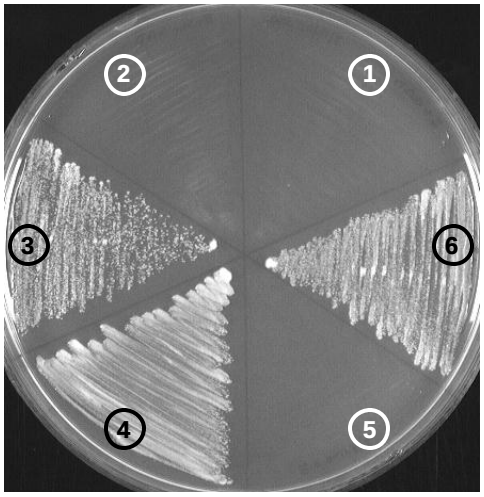

	MEI-9	GAD	growth
1	-	empty	-
2	+	empty	-
3	-	MEI-9	+
4	+	MEI-9	+
5	-	MUS312	-
6	+	MUS312	+

Figure 2.6. Yeast two-hybrid assay with ERCC1, MUS312, and MEI-9. ERCC1 was expressed in yeast as a fusion protein with the *Gal4* DNA-binding domain (GBD) in a vector that either did (2,4,6) or did not (1,3,5) also express MEI-9. Yeast were transformed with an empty *Gal4* activation domain (GAD) vector (1,2), a vector expressing GAD-MEI-9 fusion protein (3,4), or GAD-MUS312 fusion protein (5,6). Growth on the –HIS dropout media pictured indicates an interaction between the GBD- and GAD- fusion proteins.

We found that ERCC1 and MUS312 do not interact directly in a yeast two-hybrid assay; however, expression of untagged MEI-9 protein in the same yeast two-hybrid assay does allow ERCC1 and MUS312 to interact (Figure 2.6). This is the first evidence for all three proteins participating in a complex simultaneously.

ERCC1 is required for a subset of meiotic crossovers: We have shown that the *Ercc1*^{X} somatic phenotype is identical to that of a *mei-9* mutant, but that the meiotic phenotype is less severe than that of *mei-9*. Our two models for MEI-9

complex formation predicted that either ERCC1 would be required for meiotic recombination to the same extent as MEI-9 and MUS312 (MEI-9-ERCC1-MUS312 is the functional meiotic complex) or that ERCC1 would not be required for meiotic recombination at all (MEI-9-MUS312 is the functional meiotic complex.) Our results show that ERCC1 is required for generating some crossovers, but not as many as MEI-9. This suggests that MEI-9-ERCC1-MUS312 functions to generate most crossovers, but MEI-9-MUS312 is sufficient without ERCC1 to generate a small number of crossovers. It is unclear whether the crossovers that remain in an *Ercc1* mutant represent a special class of crossovers that are normally generated by a MEI-9-MUS312 complex or whether these crossovers are normally generated by a MEI-9-ERCC1-MUS312 complex. We also cannot rule out the possibility that some meiotic crossovers may require ERCC1 but not MEI-9; however, we have determined that not all of the residual crossovers in *mei-9* mutants require ERCC1 because in a *mei-9 Ercc1* double mutant, some crossovers remain (data not shown). Whether ERCC1 is required only for generating certain types of crossovers or whether MEI-9-MUS312 is able to function less efficiently without ERCC1 will be explored by investigating biochemical activities of these proteins.

MATERIALS AND METHODS

Drosophila stocks and genetics: Genetic loci not described in the text are described in FlyBase (DRYSDALE *et al.* 2005). Flies were reared on standard medium at 25°.

Sensitivity to killing by ultraviolet (UV) light was assessed by collecting embryos on grape agar plates overnight, aging to third instar larvae (about four days), and then spreading larvae into a monolayer on chilled petri plates. Larvae were irradiated in a Stratalinker (Stratagene, La Jolla, CA). Sensitivity to methyl methanesulfonate (MMS) was assessed by allowing adults to lay eggs in plastic vials for two days and, after one additional day, adding 250 µL of 0.025%, 0.05%, or 0.075% solution of MMS in water to the food. For *Ercc1*^{X} homozygous and hemizygous crosses, *Ercc1*^{X}*/CyO* females were crossed to *Ercc1*^{X}*/Df(2R)knSA3* males. For *mei-9*^{A2} crosses, *mei-9*^{A2}*/FM7* females were crossed to *mei-9*^{A2} males. Percentage survival is calculated as the treated ratio of mutant to control flies divided by the untreated ratio of mutant to control flies. Means and standard deviations were determined from at least three independent experiments.

For the *X* chromosome nondisjunction assay, female flies of the appropriate genotype were crossed to *C(1;Y)1, v f B/O* males. Progeny from normal disjunction are Bar females (*X/C(1;Y)1, v f B*) and non-Bar males (*X/O*). Half of the diplo-*X* progeny survive as non-Bar females (*X/X*) and half die (*X/X/C(1;Y)1, v f B*). Half of the nullo-*X* progeny survive as Bar males (*C(1;Y)1, v f B/O*) and half die (*O/O*). The percentage of *X* chromosome nondisjunction is calculated as twice the number of viable exceptional progeny divided by the total of normal progeny plus twice the number of exceptional progeny.

Direct measurements of crossing over on the 3rd chromosome were performed in flies of the appropriate genotype and heterozygous for mutations in *Ly*

st ry and *e*. Map distance is calculated as 100 times the number of recombination events in the interval divided by the total number of flies. For zygotic *Ercc1*^{X} and *mei-9*^{A2} mutants, mutant females tested were derived from heterozygous mothers. For maternal/zygotic mutants, mutant females tested were derived from homozygous mutant mothers.

P element constructs and germline transformation: The transformation vector p*P*{Target} was built from pCaSpeR4 (PIRROTTA 1988), and carries the *w*$^{+mC}$ marker from that vector. The FRT sequences are derived from oligonucleotides containing the 34-bp minimal sequence. For the derivative p*P*{TargetB}, the 3' half of *white* was replaced with cDNA sequences, resulting in removal of introns 3-5 and of sequences downstream of the translation termination site. The vectors and complete sequences are available from the Drosophila Genomic Resources Center (http://dgrc.cgb.indiana.edu).

For the targeting construct p*P*{*Ercc1*^{X}}, the *Ercc1* region was amplified as two PCR products. The left product contained -2158 to 291 (using the ATG at the beginning of the *Ercc1* coding region as +1). The primer within *Ercc1* included two extra base pairs to generate an *Xho*I site, which was used to clone this fragment into a plasmid vector. Similarly, the right product extended from 288 to 2614, and the primer within *Ercc1* included two extra base pairs to generate an *Xho*I site. When cloned into the construct carrying the left half, a genomic region of 4.8 kb was produced, with a 2 bp insertion in *Ercc1* generating a frame-shift mutation marked by an *Xho*I site. An *I-Sce*I recognition sequence was inserted into the

unique *Nsi*I site in the 3' untranslated region of *Ercc1* by annealing two oligonucleotides that generated the desired sequence and overhangs compatible with *Nsi*I-digested DNA. This fragment was cloned into p*P*{Target}.

To generate *P*{*WUF9*}, a 1886-bp fragment of the 5' end of *Ubiquitin*, containing the first, non-coding exon, the first intron, and the first 11 bp of the second exon, was cloned into pBluescript KS+. Oligonucleotides encoding an initiator methionine and the FLAG epitope (DYKDDDDK) were added to generate pBUF (Bluescript-*Ubiquitin*-FLAG). The complete coding sequence from a *mei-9* cDNA (as reported in SEKELSKY *et al.* 1995) was cloned into this vector, and the entire module was then transferred into pCaSpeR4 to generate p*P*{*WUF9*} (*white-Ubiquitin*-FLAG-*mei-9*). The *mei-9* cDNA used to create this construct encodes a 926 amino acid protein. Version 3.2 of the *Drosophila* genome reports a *mei-9* cDNA that encodes a 961 amino acid protein, with 35 amino acids added at the N terminus; however, these 35 amino acids have no homology to other proteins related to MEI-9, and this *P*{*WUF9*} construct rescues *mei-9* mutant phenotypes (data not shown), indicating that the extra amino acids are not essential to MEI-9 function.

Homologous gene targeting: We conducted gene targeting according to the method of Rong *et al.* (2002), with the following modifications: females carrying the targeting construct and the *I-Sce*I and FLP transgenes were crossed to males homozygous for a transgene expressing FLP constitutively, in bottles. Rare progeny with colored eyes were then crossed to generate stocks and to map the insertion to

a chromosome. Of three inserts on chromosome *2*, one was determined by PCR to be within *Ercc1* (Figure 2.3). The other two were determined genetically to be unlinked to *Ercc1*.

Molecular Analysis of Ercc1^{X}: To generate the *Ercc1^{X}* allele, we recovered viable reductions of the targeted duplication over a deficiency for the region and then analyzed these events by PCR followed by *Xho*I digestion. Fly DNA was prepared by homogenization in buffer and incubation with proteinase K (GLOOR *et al.* 1993). PCR was done using a forward primer at -67 (numbers are relative to the start of *Ercc1* translation) (5'-GTGCCTTCGTCACCTGATA-3') and a reverse primer at 700 (5'-GGCAGCATCAGTCTTGTTC-3'). Following digestion, products were analyzed on agarose gels. The presence of *Ercc1* generates a 769 bp PCR product, while the presence of *Ercc1^{X}* generates two cleaved products of 414 bp and 355 bp and the presence of both alleles generates all 3 products. One of the four viable reductions recovered had only the two smaller products and so has only the *Ercc1^{X}* allele.

Allele-specific PCR was designed with primers to the region of *Ercc1* in which the *Xho*I site was inserted. The forward primer at 274 to amplify *Ercc1* is 5'-GATTA TGTGGTCGGTCGAAC-3' and to amplify *Ercc1^{X}* is 5'-GATTATGTGGTCGGCTCGAG-3'. These primers were used in combination with a reverse primer at 2655 (5'-GCCACAC TCCGGATCTTCTG-3') on wild-type, targeted duplication, and *Ercc1^{X}* flies. We confirmed that the *Ercc1^{X}* primer does not amplify *Ercc1*, that the targeted duplication contains an ~1.6 kb deletion downstream of the *Ercc1^{X}* allele, and that *Ercc1* is not present in *Ercc1^{X}*; however, we also unexpectedly recovered an ~1.2 kb

product from *Ercc1*^{X} flies. Sequencing of this product revealed vector sequence expected to have been removed by the reduction.

To determine the genomic sequence surrounding the remaining vector sequences, we did PCR using a forward primer at 1990 (5'-CCCATTGATGGTCAAGT GCT-3') and a reverse primer complementary to the *I-Cre*I site in the vector sequence (5'-GACCAAACTGTCTCACGACGTTTTG-3') and a second PCR using a forward primer complementary to the *I-Cre*I site (5'-CGTCGTGAGACAGTTTGGT-3') and the reverse primer at 2655 (see above). These PCR products were sequenced, showing that from 1990 through to the *I-Cre*I site, the genomic sequence is identical to that of the targeted duplication, while from the *I-Cre*I site through to 2655, 6279 bp of vector sequence, including most of the *white* gene, is deleted relative to the targeted duplication.

To ensure that *Ercc1*^{X}, which we have shown to be the only *Ercc1* allele present, is upstream of this remaining vector sequence, we did a PCR reaction using a forward primer at 217 (5'-CCCATCCTGAAATCCATACT-3') and the reverse primer to the *I-Cre*I site (see above). This reaction was sequenced and showed the presence of the inserted *Xho*I site. The resulting *Ercc1*^{X} allele is pictured graphically in Figure 2.2D.

Western blotting: Ovaries were dissected on ice from *Drosophila* females of the genotypes described in the text. The ovaries were then boiled and sonicated in SDS sample buffer prior to loading onto a polyacrylamide gel at the equivalent of one pair of ovaries per lane. After separation by electrophoresis, proteins were

transferred to polyvinyl difluoride (PVDF) membrane. MEI-9 was detected with rabbit polyclonal anti-MEI-9 serum, using the ECL detection kit (Amersham, Arlington Heights, IL).

Yeast two-hybrid assay: We used the two-hybrid system described in James *et al.* (1996) with a modification to the pGBD fusion plasmid that inserts a second multiple cloning site flanked by a *Gal4* promoter and transcription and translation start sites and an *Adh1* 3' UTR (pGBT61, M. Nichols, personal communication). This vector allows expression of an untagged protein that can act as a bridge in the yeast two-hybrid assay. Full-length *Ercc1* cDNA sequence was cloned into the *Nco*I and *Pst*I sites in pGBT61 to create pGBT61-*Ercc1*. Full-length *mei-9* cDNA sequence (as reported in SEKELSKY *et al.* 1995) was cloned into the *Stu*I and *Kpn*I sites in pGBT61-*Ercc1* to create pGBT61-*Ercc1*+*mei-9*. We obtained pGAD-*mei-9* from the *Drosophila* Genomics Resource Center, Bloomington, IN. Full-length *mus312* cDNA sequence was cloned into the *Nco*I and *BamH*I sites in pGAD (J.R. LaRocque, unpublished data).

CHAPTER 3

HETERODUPLEX DNA IN MEIOTIC RECOMBINATION IN *mei-9* MUTANTS

Accurate chromosome segregation during meiosis requires crossovers (COs) between homologous chromosomes, which are generated through meiotic recombination. A number of CO-defective mutants have been identified in model organisms (reviewed in MCKIM *et al.* 2002; VILLENEUVE and HILLERS 2001). Much of our understanding of the molecular mechanism of meiotic recombination comes from studies of the meiotic phenotypes of these mutants and the molecular cloning and functional identification of the genes involved. This analysis has led to the establishment of the double-strand break repair (DSBR) model for meiotic recombination (Figure 3.1) (SZOSTAK *et al.* 1983).

Crossovers are an important product of meiotic recombination because they ensure proper chromosome segregation; however, meiotic recombination can also result in non-crossover (NCO) products. COs are easily recognized because of the exchange of flanking markers, but NCOs can only be distinguished from non-recombinant chromosomes when accompanied by gene conversion (GC). According to the DSBR model, GC results from the repair of mismatches in heteroduplex DNA (hDNA), DNA in which each strand of the duplex is derived from a different parental chromosome.

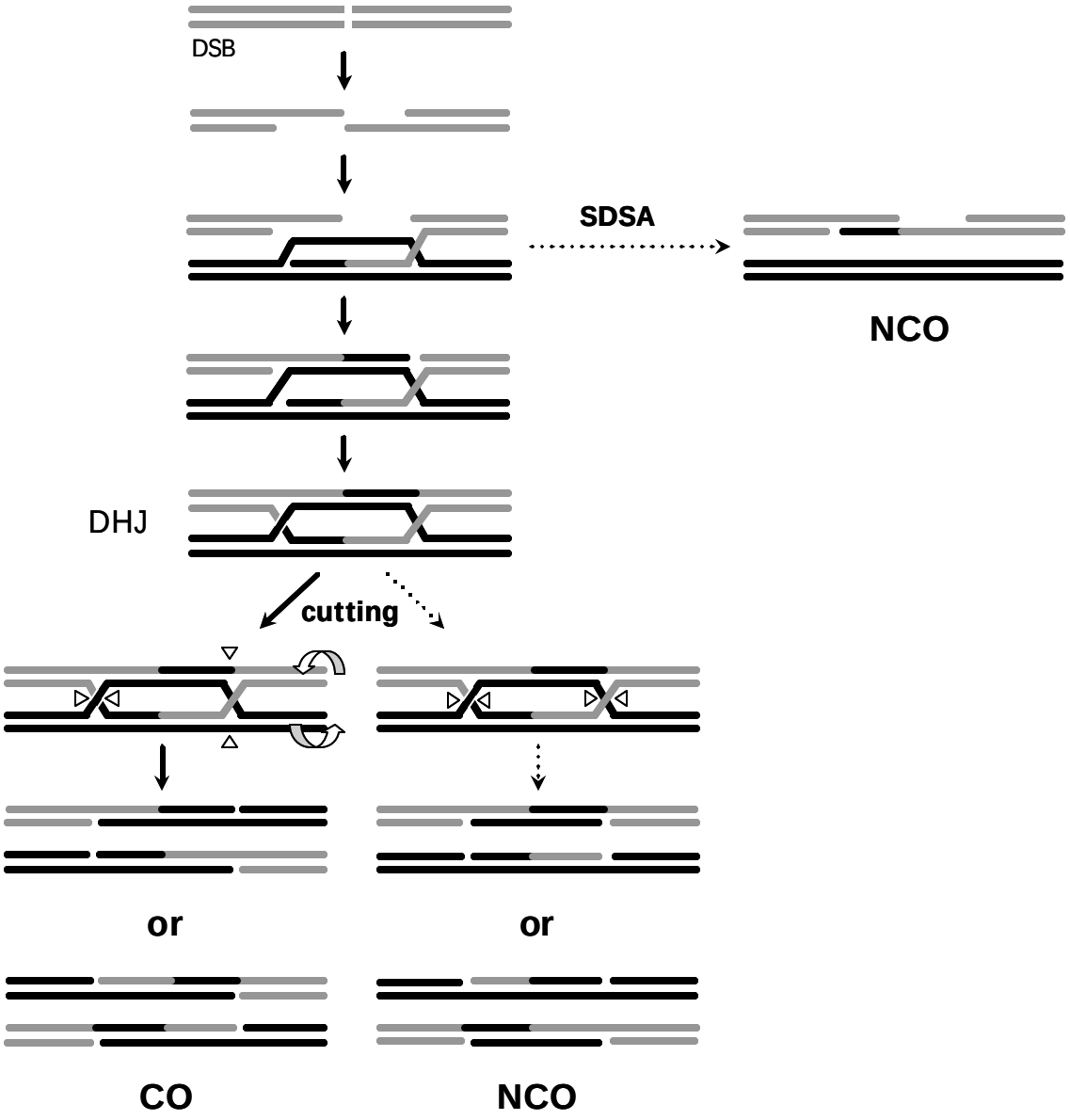

Figure 3.1. DSBR model for meiotic recombination. According to this model, recombination initiates with the introduction of a double strand break (DSB) on one chromatid (gray lines), followed by 5' to 3' resection of the ends to leave 3' single-stranded overhangs. One 3' end invades the duplex of a chromatid of the homologous chromosome (black lines), base pairing with the complementary strand and displacing the other strand as a D-loop. Synthesis follows, primed by the 3' end of the broken chromosome and using the invaded chromosome as a template. This strand either

dissociates, re-annealing to the second broken end to generate a NCO by SDSA, or, alternatively, the D-loop anneals to the second free 3' end and additional synthesis and ligation produces the double Holliday junction intermediate (DHJ). The DHJ is resolved by cutting to generate CO or NCO products.

The canonical DSBR model suggests that COs and NCOs are alternate outcomes of resolution of a common recombination intermediate, the double-Holliday junction (DHJ) structure (Figure 3.1). The existence of a class of mutations that decrease the number of COs but not the number of NCOs argues against this feature of the model. This class includes mutations in *MUS81*, *MMS4*, *MSH4*, *MSH5*, and *MLH1* in *Saccharomyces cerevisiae* (DE LOS SANTOS *et al.* 2003; DE LOS SANTOS *et al.* 2001; HOLLINGSWORTH *et al.* 1995; HUNTER and BORTS 1997; ROSS-MACDONALD and ROEDER 1994) and *mei-218*, *rec*, and *mei-9* in *Drosophila* (BLANTON *et al.* 2005; CARPENTER 1982). Analysis of these mutants suggests that there is a split in the recombination pathway with one branch leading to COs and the other to NCOs; these mutants are defective in the CO-specific branch. In fact, most NCOs in *S. cerevisiae* are now thought to be derived not from the DHJ intermediate, but from synthesis-dependent strand annealing (SDSA), with the DHJ being resolved primarily into COs (Figure 3.1) (ALLERS and LICHTEN 2001a).

Interestingly, although the number of NCOs is not decreased in these CO-defective mutants, NCOs are altered in some of them (BLANTON *et al.* 2005; CARPENTER 1982; HUNTER and BORTS 1997). One possible explanation is that these proteins are involved in both CO and NCO branches, perhaps each performing two separate functions. Alternatively, these proteins may function solely in the CO branch, and the

effect on NCOs may be a consequence of an inability to complete the CO pathway. Regardless of which hypothesis is true, further investigation of the effect on NCOs in these mutants can provide insight into the function of these proteins as well as the molecular mechanism of meiotic recombination. We have recently reported analysis of NCOs in *Drosophila rec* mutants (BLANTON *et al.* 2005). The average length of GC tracts among NCOs is lower in *rec* mutants than in wild-type, suggesting that REC facilitates repair synthesis during meiotic recombination, and that, as is thought to be the case in *S. cerevisiae*, most NCOs in *Drosophila* arise through SDSA.

Mutations in *mei-9* have a different effect on NCOs: post-meiotic segregation (PMS) has been detected in these NCOs (BHAGAT *et al.* 2004; CARPENTER 1982; CARPENTER 1984; HILLIKER and CHOVNICK 1981; ROMANS 1980b). PMS arises from a failure to repair mismatches in hDNA, resulting in sister chromatids containing different sequence information after the first round of post-meiotic replication.

Molecular cloning of *mei-9* revealed that it encodes the *Drosophila* ortholog of mammalian XPF and *S. cerevisiae* Rad1p (SEKELSKY *et al.* 1995), the catalytic subunits of DNA structure-specific endonucleases required for nucleotide excision repair (BARDWELL *et al.* 1994; PARK *et al.* 1995). This led to the hypothesis that MEI-9 nicks Holliday junctions, resolving the DHJ into CO products (SEKELSKY *et al.* 1995); however, this hypothesis only addresses the CO defect. We suggest two alternative hypotheses to explain the PMS phenotype: a one-function model and a two-function model. In the one-function model, the CO defect and PMS phenotype in *mei-9* mutants both result from loss of a single MEI-9 function in meiosis.

Recombination events that are blocked in the CO pathway in *mei-9* mutants instead utilize an alternative pathway that leads to a NCO with PMS. In the two-function model, the PMS phenotype of *mei-9* mutants is independent of the CO defect. PMS results from a failure to repair mismatches in hDNA, suggesting that MEI-9 is involved in meiotic mismatch repair (MMR). In fact, all known mutations that cause PMS in *S. cerevisiae* are in genes encoding MMR proteins (HUNTER and BORTS 1997). In support of this two-function model, extracts from embryos mutant for *mei-9* have defects in some types of MMR *in vitro* (BHUI-KAUR *et al.* 1998).

The two-function model proposes that MEI-9 plays a role in MMR, but within this model there are two possibilities: MEI-9 is absolutely required for MMR or MEI-9 facilitates/is partially required for MMR. The first possibility predicts that all NCOs in *mei-9* mutants would exhibit PMS. In fact, previous experiments have shown quite high levels of PMS in *mei-9* mutants, perhaps approaching 100% (BHAGAT *et al.* 2004; CARPENTER 1982). Both the second possibility and the one-function model, on the other hand, predict that there would be a class of NCOs in *mei-9* mutants that do not exhibit PMS and would be identical to wild-type NCOs. The structure and arrangement of hDNA in the PMS NCOs distinguish the second possibility from the one-function model. Indeed, these models all predict that the arrangement of hDNA in the PMS events in *mei-9* mutants can provide insight into the molecular mechanism of meiotic recombination.

To test these models, we undertook the molecular analysis of recombination events in *mei-9* mutants. We report here that the majority of NCOs in *mei-9*

mutants do not exhibit PMS. We also show that the arrangement of hDNA in the NCOs that exhibit PMS provides strong evidence for the one-function model, with the blockage in *mei-9* mutants occurring at the DHJ. This is consistent with our initial hypothesis that the function of MEI-9 during meiotic recombination is to nick Holliday junctions to generate COs.

RESULTS

To distinguish between the two-function and one-function models for the role of MEI-9 in meiotic recombination, we recovered recombination events within the *rosy* (*ry*) locus using a procedure developed by Chovnick and colleagues (CHOVNICK *et al.* 1970; CHOVNICK *et al.* 1971). The *ry* gene encodes xanthine dehydrogenase (XDH), which is required both for the metabolism of purine and normal eye pigmentation. Females *trans*-heterozygous for ry^{531} and ry^{606}, point mutations separated by 3.8 kb, were crossed to males homozygous for ry^{506}, which deletes much of the gene. Rare rosy+ recombinants were selected by treating the larvae with purine; flanking markers were used to distinguish COs from NCOs (see Materials and Methods for details).

Most NCOs from mei-9 mutants do not exhibit PMS: The two-function model which proposes that MEI-9 is absolutely required for meiotic MMR and independently required for CO formation, predicts that all NCOs from *mei-9* mutants will exhibit PMS. PMS results when mismatches in hDNA are left unrepaired after meiosis. When unrepaired hDNA is present in a gamete, DNA replication in the first zygotic S

phase will produce two different daughter molecules, which will segregate into the two daughter cells at mitosis. In a metazoan such as *Drosophila*, PMS gives rise to an individual that is mosaic, with some cells having the sequence from one strand of the recombinant chromatid and the other cells having the sequence from the other strand. In our experiment, this mosaicism manifests as recombinants with the maternal chromosome having a *ry*+ sequence in some cells and a *ry*- sequence in others. XDH is secreted and diffuses throughout the larva, allowing *ry*+//*ry*- mosaics to survive purine treatment and develop into adults that are rosy+ in eye color (ROMANS 1980a).

We used three assays to screen rosy+ adults for the presence of a maternal *ry*-sequence. First, we mated the rosy+ recombinants to ry^{506} partners and looked for transmission of a maternal *ry*- chromosome to progeny, which would indicate that the germline was either *ry*+//*ry*- mosaic or entirely *ry*-. Because this method detects only a subset of PMS events (CARPENTER 1982), we also used molecular methods. PCR of the original recombinant fly was performed using allele-specific primers designed to amplify specifically either *ry*+ or *ry*- sequence: amplification with both primers signifies PMS. These first two methods detect PMS of the *ry* missense mutations; however, it is possible to have full conversion of one of these mutations flanked by unrepaired hDNA. There are multiple heterologies between the ry^{531} and ry^{606} chromosomes that could be included in this hDNA and therefore exhibit PMS (BLANTON *et al.* 2005; HILLIKER *et al.* 1991). To detect these events, we sequenced bulk PCR products amplified with non-allele-specific primers from the

original recombinant fly and examined chromatograms for the presence of double peaks at sites of heterology between the parental chromosomes.

We previously reported analysis of 81 COs and 31 NCOs from wild-type females in which we did not detect PMS (BLANTON *et al.* 2005) (Table 3.1). We screened an additional 1.4 million larvae from wild-type females and recovered 31 COs and 22 NCOs, none of which exhibited PMS. This confirms earlier experiments that showed PMS is exceedingly rare among NCOs in wild-type *Drosophila* (CHOVNICK *et al.* 1971). We screened 1.4 million larvae from *mei-9* mutant females and recovered five COs and 32 NCOs. These rates – 90% decrease in COs and 60% increase in NCOs – are similar to those previously reported (CARPENTER 1982; ROMANS 1980b). We did not detect PMS by any of the three methods described above in any of the five COs, and we detected PMS in only five of the 32 NCOs from *mei-9* mutants. These results do not support an essential requirement for MEI-9 in MMR, but instead support either the one-function model – that PMS results from failure to generate a CO when MEI-9 is absent – or an occasional requirement for MEI-9 in meiotic MMR.

TABLE 3.1. Intragenic Recombination in Wild-type and *mei-9* Mutants

Genotype	Progeny Screened	Crossovers		Noncrossovers	
		n	Frequency	*n*	Frequency
wild-type[1]	3,710,000	112	3.0×10^{-5}	53	1.4×10^{-5}
mei-9	1,405,000	5	0.36×10^{-5}	32	2.3×10^{-5}

[1]Data from this study and (BLANTON *et al.* 2005).

Most non-PMS NCOs from mei-9 mutants are indistinguishable from NCOs from wild-type: An essential requirement for MEI-9 in MMR predicts that all NCOs from *mei-9* mutants will exhibit PMS; however, unrepaired hDNA is only detectable as PMS when it contains a mismatch. If hDNA tract length is decreased in *mei-9* mutants, we might detect less PMS than expected because the hDNA is less likely to contain a polymorphism that would cause a mismatch. GC can result from the repair of mismatches in hDNA and so increases or decreases in GC tract length can be used to infer changes in hDNA tract length; therefore, based on the level of PMS that we detected in *mei-9* mutants, an essential requirement for MEI-9 in MMR predicts that the non-PMS NCOs would have shorter GC tracts than wild-type.

We chose ry^{531} and ry^{606} for this experiment because of the presence of multiple heterologies surrounding each mutation (BLANTON *et al.* 2005; HILLIKER *et al.* 1991). This allowed us to map GC tracts in NCOs from wild-type and *mei-9* mutants at a high resolution. We previously reported the GC tracts from 29 NCOs from wild-type (BLANTON *et al.* 2005). We mapped a further 22 GC tracts from wild-type and 27 GC tracts from *mei-9* mutants (Figure 3.2). We utilized the same strategy that was used previously for determining the mean GC tract length (BLANTON *et al.* 2005). Statistical analysis showed that the mean GC tract length in NCOs from *mei-9* mutants is significantly longer than wild-type (509 bp vs. 425 bp, p=0.03); therefore, it is unlikely that the reason we see low levels of PMS in *mei-9* NCOs is because hDNA tract length is decreased. Again, this result does not support an essential requirement for MEI-9 in MMR.

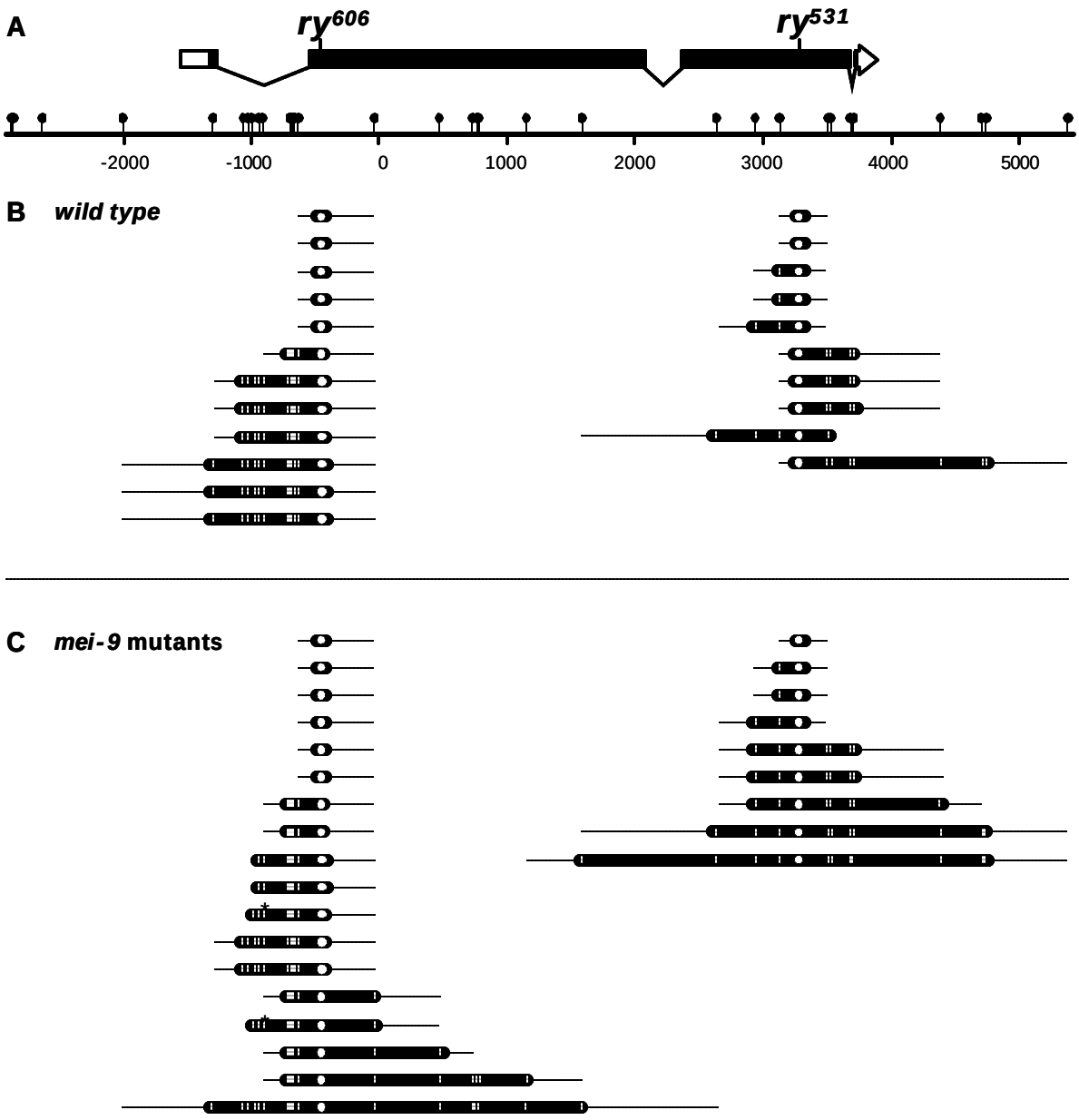

Figure 3.2. GC tracts from wild-type and *mei-9* mutants. (A) Schematic of the *rosy* locus. Intron/exon structure is shown, with coding sequences filled. The positions of the selected sites corresponding to the ry^{606} and ry^{531} chromosomes are indicated as lollipops on the scale bar. These are all single nucleotide polymorphisms, except for -1029 and -685, which are insertions of one- and four-bp, respectively in ry^{531} relative to ry^{606}. The scale is in bp, using the coordinate system of Bender *et al*. (BENDER *et al.* 1983). (B and C) Tract lengths observed in NCOs recovered from wild-type (B) and *mei-9* mutants (C).

Each bar represents an independent event, with the open circle denoting the selected marker (ry^{606} or ry^{531} mutant sites). Black bars represent the minimum tract length for each event, with co-converted sites marked by the white lines. Dotted lines represent the maximum tract length possible based on the next unconverted polymorphism. The asterisks mark two instances in which conversion at the -937 polymorphism was discontinuous (see Materials and Methods).

Closer examination of the GC tracts from *mei-9* mutants reveals that there are two that are much longer than the others (Figure 3.2, bottom GC in each column). In fact, computing an average length and standard deviation using the midpoint between polymorphisms contained within and excluded from each tract shows that the lengths of these two tracts fall more than two standard deviations from the mean (mean = 1076 bp, standard deviation = 1026 bp, lengths >3700 bp). It is possible that these extremely long GC tracts arose from recombination events in which the CO pathway was attempted, but was unsuccessful due to the absence of MEI-9, but we cannot eliminate the possibility that MEI-9 plays a role in controlling GC tract length. Excluding the two aberrant tracts, the mean unselected lengths of GCs from *mei-9* mutants (417 bp) and wild-type (425 bp) are not significantly different (p=0.8). These results show that most NCOs from *mei-9* mutants are indistinguishable from NCOs from wild-type. This suggests that most or all NCOs are MEI-9-independent.

PMS NCOs from mei-9 mutants exhibit trans hDNA: An important distinction between a partial requirement for MEI-9 in MMR and the one-function model is in the origin of the PMS NCOs. In the former, the PMS NCOs represent recombination

events that were fated to become NCOs regardless of the presence or absence of MEI-9 activity and so were generated through the usual NCO pathway(s). In contrast, in the one-function model, the PMS NCOs arise from recombination events that were fated to become COs, but were blocked from doing so by the absence of MEI-9 activity and were instead funneled into an alternative pathway to become NCOs. This alternate pathway may either be only used in the absence of MEI-9 or it may be used more often in the absence of MEI-9 than in wild-type.

The structure and arrangement of hDNA in recombination intermediates or products can be used to distinguish between models for NCO formation (Figure 3.1 and 3.4). A partial requirement for MEI-9 in MMR predicts that the PMS events from *mei-9* mutants would have hDNA structures representative of the hDNA present in NCO recombination intermediates from wild-type. In contrast, the one-function model predicts that the PMS events from *mei-9* mutants would have hDNA structures that are different from the hDNA present in NCO recombination intermediates from wild-type.

By sequencing PCR products from the mosaic flies and their progeny, we determined the arrangement of hDNA in each of the PMS NCOs. Based on this arrangement, we classified the five PMS events from *mei-9* mutants into two types (Figure 3.3). The first type includes three events that each have two adjacent hDNA tracts in the *trans* configuration. One of these also had full GC at a single polymorphic site bridging the two hDNA tracts. The second type includes two events that each have a single hDNA tract adjacent to full GC at a single site.

Unfortunately, it is not possible to compare these hDNA structures to those of NCO intermediates from wild-type flies, because in wild-type flies, the informative hDNA is repaired prior to the recovery of NCOs. However, we have characterized recombination events from a mutant lacking the MMR gene *Msh6* (Chapter 4), and these events exhibit much higher rates of PMS (Table 4.1). Additionally, the majority of the GC and hDNA tracts do not correspond to the two types of hDNA structures we recovered from *mei-9* mutants (Figure 4.2). This supports the one-function model for MEI-9, suggesting that the PMS NCOs from *mei-9* mutants are generated by an NCO pathway that is followed when recombination intermediates are prevented from becoming COs because MEI-9 is absent.

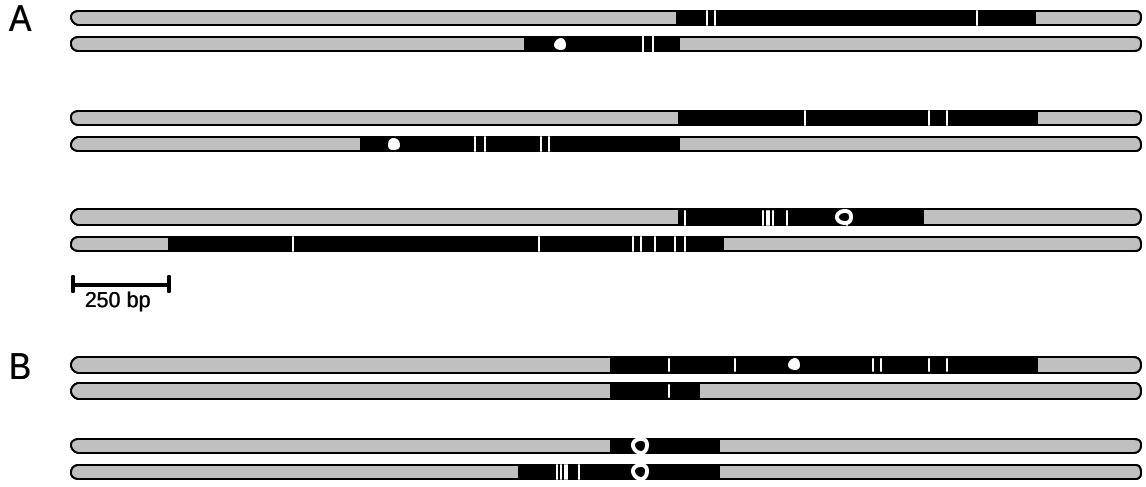

Figure 3.3. hDNA tracts from meiotic recombination in *mei-9* mutants. Each pair of bars represents the two strands of a recombinant chromosome with unrepaired hDNA. Black segments are sequences derived from the homologous chromosome, with white hatches showing positions of polymorphisms within hDNA and conversion tracts. The position of the ry^{531} point mutation is denoted by a filled white circle, ry^{606} by an open white circle. The ends of the black segments are drawn at the midpoints between the last included

polymorphism and next excluded polymorphism. (A) Three events with *trans* hDNA. In all three cases, hDNA on each side was extensive (245-1530 bp) and included at least three polymorphisms. One event showed full conversion of a single polymorphism between regions of hDNA. (B) Two events with a single hDNA tract. In both cases, a single, fully-converted polymorphism is present at one end of the tract.

DISCUSSION

Several models have been proposed to describe the molecular steps involved in CO formation, including the Holliday model (HOLLIDAY 1964), the Meselson and Radding model (MESELSON and RADDING 1975), and the DSBR model (SZOSTAK *et al.* 1983). In *S. cerevisiae* and *Schizosaccharomyces pombe*, the DSBR model is supported by physical detection of DSBs and recombination intermediates (ALLERS and LICHTEN 2001b; CERVANTES *et al.* 2000; COLLINS and NEWLON 1994; SCHWACHA and KLECKNER 1994; SCHWACHA and KLECKNER 1995). In multicellular organisms, meiosis typically occurs asynchronously in a small subset of cells in the gonad, making detection of DSBs and recombination intermediates through physical assays technically difficult or impossible; therefore, no such evidence to support the DSBR model exists in *Drosophila*.

Despite this lack of physical evidence, it seems likely that the general features of the DSBR model can be applied to *Drosophila* because many of the proteins involved in the early stages of meiotic recombination are conserved, including an ortholog of the protein that catalyzes DSB formation in yeast (MCKIM and HAYASHI-HAGIHARA 1998). Without a direct link between DSBs and the initiation of meiotic

recombination in *Drosophila*, however, we must consider the nick-initiated models of Holliday and Meselson and Radding as formal possibilities. To gain insight into the molecular mechanism of CO formation in *Drosophila*, we investigated recombination in the CO-defective mutant, *mei-9*.

Although the number of COs is severely decreased in *mei-9* mutants, the number of NCOs is not decreased, suggesting that MEI-9 is required in a CO-specific branch of the meiotic recombination pathway. NCOs are not unaffected, however: in *mei-9* mutants, some NCOs exhibit PMS. Our results support a model in which MEI-9 has a single function in meiosis: to generate COs from a recombination intermediate. In the absence of MEI-9, this intermediate is resolved through another mechanism to generate NCOs that exhibit PMS. The arrangement of hDNA within the PMS events can be used to infer from which step of recombination this diversion occurs, and hence which part of the pathway is blocked through loss of MEI-9 function.

We observed two types of PMS events from *mei-9* mutants: *trans* hDNA and full GC with one hDNA tract (Figure 3.2). These two types of PMS events may arise from two different NCO pathways used in the absence of MEI-9. Another possibility is that all five PMS NCOs are derived from an NCO pathway that generates *trans* hDNA, but that we have failed to detect *trans* hDNA in two cases. We may fail to detect *trans* hDNA if one tract does not include a polymorphism. Based on the nearest polymorphism adjacent to the full GC tract, the unrepaired hDNA would have to have been less than 304 bp in one case and less than 424 bp in the other

(Figure 3.2B). These are both within two standard deviations of the mean hDNA tract length computed using the midpoint between polymorphisms contained and excluded within each of the eight hDNA tracts detected (mean = 805 bp, standard deviation = 381 bp); therefore, we cannot exclude the possibility that in these two cases the second hDNA tract was so short that it did not include a polymorphism.

We may also fail to detect *trans* hDNA if one tract undergoes repair that restores the sequence originally on that chromatid. If each of the tracts in a molecule with *trans* hDNA can be repaired independently, and there is no bias toward restoration repair, we would predict that we would observe an additional type of PMS event: one in which one of the hDNA tracts underwent conversion repair to generate an extensive region of full GC flanked by a single hDNA tract. Given the small sample size (n=2), failure to observe this type of PMS event cannot be interpreted as evidence against the independent repair of hDNA tracts. If independent repair can occur, we would also predict that we would observe events in which both tracts of the *trans* hDNA underwent conversion repair to generate extensive GC tracts. This is a possible explanation for the two unusually long GC tracts we observed among NCOs from *mei-9* mutants.

To infer from which step recombination is diverted in a *mei-9* mutant, we must consider the possible sources of the PMS events that we observed. The *trans* hDNA that we observe in PMS NCOs from *mei-9* mutants is not consistent with models in which recombination is initiated by nicks, i.e., the Holliday or Meselson and Radding models, but is consistent with models in which recombination is

initiated by a DSB, because this allows both strands of the cut duplex to receive information from the homologous chromosome. Our results, therefore, provide genetic support to strengthen the case made by protein conservation for the DSBR model for CO formation in *Drosophila*.

Based on the DSBR model, four possible sources of *trans* hDNA can be envisioned: (A) two-ended SDSA; (B) cutting of the DHJ intermediate at a single HJ followed by branch migration of the second HJ through the nick; (C) branch migration of both HJs past the region of hDNA followed by resolution; and (D) branch migration of both HJs toward one another followed by decatenation by topoisomerase (DHJ dissolution) (Figure 3.4). The single, full GC polymorphism in one of the *trans* events we observed could be explained either by using a model in which recombination initiates with a gap rather than a double-strand break or if the initial strand invasion were accompanied by limited proof-reading, similar to "early repair" that has been suggested to occur in *S. cerevisiae* (ALANI *et al.* 1994). Two-ended SDSA (Figure 3.4A) is an unlikely source of the *trans* hDNA that we observed in NCOs from *mei-9* mutants because it requires the diversion from the CO pathway to occur at a very early step (Figure 3.1), contrary to evidence indicating that MEI-9 functions late in the CO pathway (BAKER and CARPENTER 1972). The other possible sources of *trans* hDNA involve diversion from a DHJ intermediate (Figure 3.4B-D), which is consistent with a late function for MEI-9.

The second type of PMS event, a single hDNA tract adjacent to a site of full conversion (Figure 3.2B), has two possible sources (in addition to the possibility that

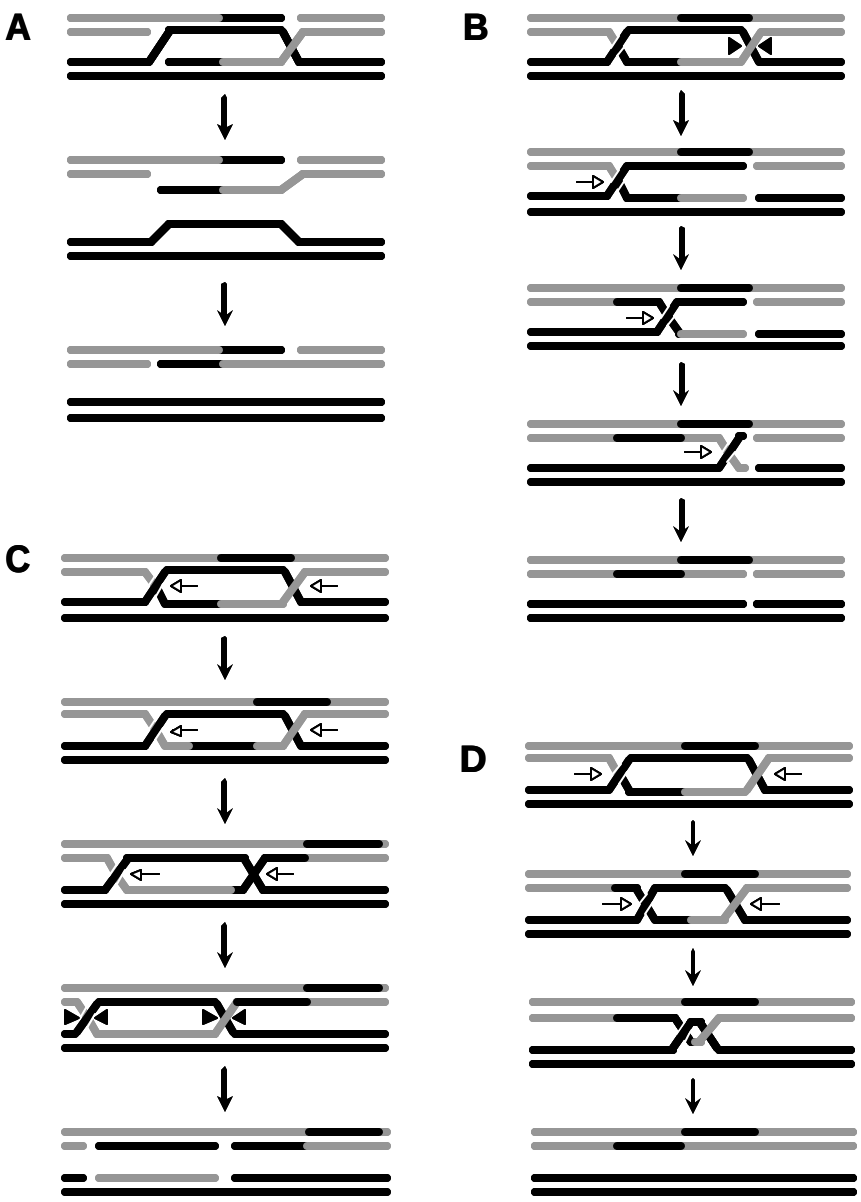

Figure 3.4. Models for the formation of *trans* hDNA. (A) According to the canonical synthesis-dependent strand annealing (SDSA) model (FORMOSA and ALBERTS 1986), after strand invasion and synthesis the nascent strand dissociates from the template and anneals to the single-stranded overhang on the other side of the DSB. Shown here is two-ended SDSA, in which both nascent strands dissociate prior to ligation and re-anneal to their original partners. (B) One Holliday junction in the DHJ is cut (black arrows) and the other is branch migrated (white arrows) through the nicks. (C) Both Holliday junctions in the DHJ are branch migrated in the same direction past the region of strand invasion and synthesis and resolved by cutting. (D) The DHJ may also undergo dissolution, which involves branch migration of the two junctions toward one another, followed by decatenation. All four models predict that one chromatid will contain *trans* hDNA, but only DHJ dissolution results in a product that does not contain nicks.

these events contain undetected *trans* hDNA): (1) SDSA accompanied by gap repair or "early MMR"; or (2) DHJ cutting (Figure 3.1). As stated above, SDSA is an unlikely source of these events because it is inconsistent with the late recombination function of MEI-9, leaving DHJ cutting as a likely candidate. Both types of PMS events, then, are consistent with a blockage at the DHJ occurring in *mei-9* mutants, suggesting that MEI-9 is required to transition this structure into COs.

An important factor to consider is that the PMS NCOs from *mei-9* mutants escape MMR. Our results indicate that MEI-9 is not directly involved in meiotic MMR, which implies that PMS in NCOs from *mei-9* mutants results from utilization of a NCO pathway that is refractory to MMR. In proliferating cells, MMR is stimulated by nicks (reviewed in KUNKEL and ERIE 2005), and it has been suggested that at least some meiotic MMR is nick-dependent (FOSS *et al.* 1999). Of the sources of *trans* hDNA enumerated above (Figure 3.4), DHJ dissolution (Figure 3.4D) is unique in that nicks are not present after the DNA strands are resolved into independent duplexes. For this reason, we favor DHJ dissolution as the source of unrepaired *trans* hDNA in NCOs from *mei-9* mutants.

Based on the homology of MEI-9 to known DNA structure-specific endonucleases and the genetic requirement for its nuclease function in generating COs (SEKELSKY *et al.* 1995; YILDIZ *et al.* 2004), we have previously proposed that the function of MEI-9 is to nick HJs (BLANTON and SEKELSKY 2004; SEKELSKY *et al.* 1998). The results reported here are consistent with this hypothesis. Furthermore, based on our analysis of hDNA in recombination products from *mei-9* mutants, we suggest

that these HJ nicks are used both to generate COs and to stimulate MMR of heterologies in hDNA, and in the absence of MEI-9, the DHJ is resolved by dissolution to produce NCOs that lack nicks to stimulate MMR.

MATERIALS AND METHODS

120 female flies homozygous for *mei-9*^{a} and *trans*-heterozygous for *ry*^{531} and *ry*^{606} were crossed to 30 male flies homozygous for *ry*^{506}. Crosses were set up in bottles containing 25 ml of standard food medium and placed at 25°. After three days, flies were transferred to fresh media to establish a second brood, and purine was added to the first brood bottles in the amount of 0.75 ml of either 0.15%, 0.18%, or 0.20% (v/v) in water. One out of every twenty-five bottles was left untreated and adult progeny were counted to estimate the number of larvae screened. Purine dosage did not grossly affect the recovery of PMS events: we recovered 1 PMS event out of 275,000 screened at 0.15%, 2 out of 525,000 at 0.18%, and 2 out of 550,000 at 0.20%. In contrast, the number of *ry* mutants that escaped killing by purine was strongly affected by purine dosage: escapers increased approximately 10-fold between 0.18% and 0.15% (data not shown).

Recombinant progeny were scored for flanking visible markers to determine whether a CO or GC event had occurred. The *ry*^{531} chromosome carried a mutation in *cv-c*, located approximately 2.1 map units distal to *ry*, and the *ry*^{606} chromosome carried a mutation in *kar*, located approximately 0.3 map units proximal to *ry*. Recombinants were then mated to *ry*^{506} flies of the opposite sex to detect mosaicism

in the germline. DNA from recombinant flies was then prepared by homogenization of the entire fly in buffer containing proteinase K, as described (GLOOR *et al.* 1993), and GC tracts were determined by PCR amplification and sequencing. The GC tracts from two NCOs from *mei-9* mutants were found to be discontinuous at the -937 polymorphism (Figure 3.2) because this marker failed to be converted like all the surrounding markers. We have previously shown evidence of discontinuity in one GC tract from wild-type (BLANTON *et al.* 2005), so we do not believe this result to be a consequence of *mei-9* mutation.

To detect PMS, allele-specific PCR primers were designed to specifically amplify mutant or wild-type sequences at the two *ry* point mutations. Primers were designed such that the 3' end corresponds to the allele-specific nucleotide. A mismatch was also engineered in the primer 2 or 3 nucleotides upstream of the 3' end to increase the specificity. Each primer set was optimized for annealing temperature and magnesium concentration. In each experiment, primers were tested against control fly preps to ensure that non-specific amplification would not produce a false positive. DNA from each recombinant was tested using the corresponding wild-type and mutant allele-specific primer sets. Amplification with both allele-specific primers indicates PMS at the *ry* allele. Allele-specific PCR products were purified and sequenced to determine the length and arrangement of hDNA tracts. Extensive tracts required additional allele-specific primers for several of the silent polymorphisms in the region. These primers were designed as described above.

Additional non-allele-specific primers were used to detect PMS accompanied by full conversion of the *ry* allele. PCR products were sequenced in bulk and the chromatogram examined for double peaks. For the single event of this type that we detected, it was not possible to design allele-specific primers to confirm the PMS and map the hDNA tracts. Instead, non-allele-specific primers were used to amplify the region, and the product was cloned into a convenient vector for amplification in *E. coli*. Clones were sequenced until we had at least one representing each strand of the hDNA region.

Mean GC tract lengths and statistical comparisons were calculated as described (BLANTON *et al.* 2005).

CHAPTER 4

MEIOTIC RECOMBINATION IN *Msh6* MUTANTS REVEALS DISCONTINUOUS GENE CONVERSION TRACTS

Crossovers (COs) generated through meiotic recombination are essential to the correct segregation of chromosomes during meiotic divisions in most eukaryotes. An understanding of the DNA transactions required to generate COs is central to the understanding of this crucial phenomenon. Several models of meiotic recombination have been proposed to describe the molecular steps required to generate COs. These models must account not only for CO formation, but also for the formation of noncrossovers (NCOs) and the association of gene conversion (GC) with both COs and NCOs.

More than forty years ago, Robin Holliday proposed a model for meiotic recombination to account for these observed phenomena (HOLLIDAY 1964). One prominent feature of this model is the suggestion that GC associated with both COs and NCOs is generated by the formation and repair of heteroduplex DNA (hDNA), DNA in which each strand of the duplex is derived from a different parental chromosome. Although several other models for meiotic recombination have been proposed over the years, invoking different initiating lesions and different

recombination intermediates, formation and repair of hDNA as a mechanism for GC has remained a constant (MESELSON and RADDING 1975; SZOSTAK *et al.* 1983).

Experimental evidence supports models in which the formation and repair of hDNA are important features of meiotic recombination. Physical characterization of recombination at a meiotic hotspot in *Saccharomyces cerevisiae* has detected hDNA in recombination intermediates (ALLERS and LICHTEN 2001b). Additionally, post-meiotic segregation (PMS) of alleles has been observed among the products of meiotic recombination. PMS occurs most frequently in mutants that abolish mismatch repair (MMR) (reviewed in BORTS *et al.* 2000) or for poorly-repaired markers, such as palindromes (NAG *et al.* 1989), suggesting that PMS arises from the failure to repair mismatches formed in hDNA during meiotic recombination.

Although the formation and repair of hDNA is a common feature of models for meiotic recombination, the structure and arrangement of hDNA present in the proposed recombination intermediates and products differs in different models. Investigation of hDNA present in the PMS products of meiotic recombination in *S. cerevisiae* has provided insights into the mechanism of CO formation (FOSS *et al.* 1999; HOFFMANN and BORTS 2005; HOFFMANN *et al.* 2005; MERKER *et al.* 2003); however, the degree to which details of the structure and arrangement of hDNA can be determined through these experiments is limited. Detection of hDNA requires the presence of heterologies between homologous chromosomes, and it has been shown that high levels of heterology in *S. cerevisiae* decrease the frequency of recombination (BORTS and HABER 1987). Levels of heterology ranging from ~0.05%

to ~0.3% have been used in experiments in *S. cerevisiae* (BORTS and HABER 1987; GILBERTSON and STAHL 1996; JESSOP *et al.* 2005; JUDD and PETES 1988; MERKER *et al.* 2003; SYMINGTON and PETES 1988); however, the highest levels of heterology have included, at most, three polymorphisms. In *Drosophila melanogaster*, high levels of heterology do not decrease the frequency of recombination (HILLIKER *et al.* 1991). We have previously studied recombination between two highly polymorphic chromosomes in *Drosophila* and have used the multiple heterologies to determine the extent of GC tracts with high resolution (Chapter 3, BLANTON *et al.* 2005).

The study of unrepaired hDNA in the PMS products of meiotic recombination in *Drosophila* provides an opportunity to gain insight into the structure and arrangement of hDNA at a high resolution. In *S. cerevisiae*, even well-repaired markers, such as base-base mismatches or small insertion/deletion loops, sometimes go unrepaired, resulting in PMS (FOGEL *et al.* 1981). Although the polymorphisms present between *Drosophila* chromosomes often cause these same types of heterologies, PMS is exceedingly rare (CHOVNICK *et al.* 1971). To analyze the structure of hDNA in meiotic recombination in *Drosophila*, we sought to decrease repair by knocking out the canonical MMR pathway.

In *E. coli*, MMR is carried out by the MutS, MutL, and MutH proteins (reviewed in MODRICH and LAHUE 1996). Eukaryotic genomes encode multiple homologs of MutS and MutL, although no homologs of MutH have been identified. The *Drosophila* genome encodes two MutS homologs, *spel1* (*MSH2* ortholog) and *Msh6*, and two MutL homologs, *Mlh1* and *Pms2* (reviewed in SEKELSKY *et al.* 2000a).

We generated deletions that remove most of the coding sequence of *Msh6*. We report here that mutation of *Drosophila Msh6* greatly increases the incidence of PMS among both CO and NCO products of meiotic recombination. This suggests that hDNA is a common feature of meiotic recombination intermediates in *Drosophila*, and that MMR homologs are important for the repair of this hDNA. Surprisingly, tracts of GC and unrepaired hDNA from *Msh6* mutants are frequently discontinuous, a phenomenon that we did not observe among wild-type CO and NCO products (data not shown, Chapter 3, BLANTON *et al.* 2005). We propose that, as has been suggested in *S. cerevisiae* (COIC *et al.* 2000), in the absence of canonical MMR, mismatches are repaired by a system that allows closely-spaced mismatches to be repaired or left unrepaired, independent of one another. Unfortunately, this alternate MMR system obscures much of the information provided by the structure and arrangement of hDNA; however, analysis of the remaining unrepaired hDNA provides insights into the mechanism of meiotic recombination in *Drosophila*.

RESULTS

Deletion of Msh6 coding sequence by P excision: In yeast and mammalian systems, MMR is carried out by two functional heterodimers of MutS homologs, MutSa (Msh2 and Msh6) and MutSß (Msh2 and Msh3). Consequently, mutations in *MSH2* and *MSH6* do not elicit equivalent phenotypes in these organisms. The *Drosophila* and *Caenorhabditis elegans* genomes encode orthologs of Msh2 (SPEL1 in *Drosophila*) and Msh6 (DENVER *et al.* 2005; SEKELSKY *et al.* 2000a), but not Msh3,

suggesting that only MutSa is present in these organisms. In support of this proposal, *C. elegans msh-2* and *msh-6* mutants have identical phenotypes with regards to mutation accumulation (DENVER *et al.* 2005).

Flores and Engels constructed a synthetic deletion of *spel1* using overlapping deletions *in trans*, together with a transgene to replace a second gene contained in the region of overlapping deletion (FLORES and ENGELS 1999). These mutants were shown to exhibit increased microsatellite instability (FLORES and ENGELS 1999), a common feature of MMR mutants in other species, suggesting that MMR function is conserved in *Drosophila*. Based on the results from *C. elegans*, we hypothesize that *spel1* and *Msh6* are equivalently required for MMR in *Drosophila*. Because *Msh6* is on chromosome *3*, it is technically easier to use mutations in this gene for characterization of unrepaired hDNA in the products of meiotic recombination.

We obtained a *Drosophila* stock in which a *P* element was inserted 43 bp upstream of the *Msh6* coding sequence, and used it to generate deletions through excision of the *P* element. Mutations in *Drosophila mus309* increase the recovery of flanking deletions following *P* element excision (ADAMS *et al.* 2003; MCVEY *et al.* 2004b), so we screened for deletions following excision in both wild-type and *mus309* mutant backgrounds. Of 153 *P* excisions from wild-type, one (0.6%) had a deletion of *Msh6* coding sequence. In contrast, of 31 *P* excisions from *mus309* mutants, four (13%) had a deletion into *Msh6* sequence, confirming that this is an effective method for increasing the recovery of deletion mutants from *P* excision screens.

Through PCR and sequencing, we determined the breakpoints of four of five *Msh6* deletions. The single deletion obtained from wild-type (*Msh6*^{11}) removed ~850 bp of the 3.8 kb coding sequence. The three mapped deletions obtained from *mus309* mutants were larger: *Msh6*^{10}, *Msh6*^{59}, and *Msh6*^{68} remove 2.2 kb, 3.8 kb, and 2.8 kb of coding sequence, respectively. This suggests that a *P* excision screen performed in a *mus309* mutant background not only increases the frequency of deletion, but also increases recovery of larger deletions.

All experiments described below were performed in the *trans* heterozygous genotype *Msh6*^{10}/*Msh6*^{68}. These alleles remove most or all of the coding sequence, so this genotype should represent a complete absence of *Msh6* activity.

Both COs and NCOs are increased in Msh6 mutants: Several MutS and MutL homologs are required for the generation of COs in *S. cerevisiae*, including Msh4, Msh5, Mlh1, and Mlh3 (BORNER *et al.* 2004; GUILLON *et al.* 2005; HUNTER and BORTS 1997; WANG *et al.* 1999). To determine whether *Drosophila* MSH6 has a role in CO formation, we recovered meiotic recombination events within the *rosy* (*ry*) locus, using a procedure developed by Chovnick and colleagues (CHOVNICK *et al.* 1970; CHOVNICK *et al.* 1971). The *ry* gene encodes xanthine dehydrogenase (XDH), which is required both for the metabolism of purine and normal eye pigmentation. Females *trans*-heterozygous for *ry*^{531} and *ry*^{606}, point mutations separated by 3.8 kb, were crossed to males homozygous for *ry*^{506}, which deletes much of the gene. Rare rosy+ recombinants were selected by treating the larvae with purine; flanking

markers were used to distinguish COs from NCOs (see Materials and Methods for details).

We previously reported the results from a screen for recombination events in wild-type in which we screened 3.7 million larvae and recovered 112 COs and 53 NCOs (Table 4.1) (Chapter 3, BLANTON *et al.* 2005). We screened 1.8 million larvae from *Msh6* mutants and recovered 67 COs and 42 NCOs, a 25% rate increase over wild-type in COs and 66% rate increase in NCOs (Table 4.1). These results show that *Msh6* is not required for the generation of COs.

TABLE 4.1. Intragenic Recombination in Wild-type and *Msh6* Mutants

Genotype	Progeny Screened	Crossovers			Noncrossovers		
		n	Frequency	PMS	*n*	Frequency	PMS
wild-type*	3,710,000	112	3.0×10^{-5}	0%	53	1.4×10^{-5}	0%
Msh6	1,775,000	67	3.8×10^{-5}	21%	42	2.4×10^{-5}	58%

*Data from (Chapter 3, BLANTON *et al.* 2005)

Our results do demonstrate a role for MSH6 in the repair of mismatches in hDNA. In a metazoan such as *Drosophila*, PMS results in a mosaic individual, with some cells having the sequence from one strand of the recombinant chromatid and the other cells having the sequence from the other strand. In our experiment, this mosaicism results in an individual in which the maternal chromosome is *ry*+ in some cells and *ry*- in others. XDH is secreted and diffuses throughout the larva, allowing *ry*+//*ry*- mosaics to survive purine treatment and develop into adults that are rosy+ in eye color (ROMANS 1980a).

If one of the *ry* point mutations is included in hDNA during recombination, MMR may either restore the *ry*- sequence or convert it to *ry*+ sequence. Restoration of *ry*- sequence will not be recovered after purine selection; however, in the absence of MMR, these potential restoration events will be recovered as *ry*+//*ry*- mosaics, leading to an observed increase in the recovery of recombinants. In our system, we recover COs that occur anywhere in the 3.8 kb between *ry* point mutations, whereas we only recover NCOs that included GC of one *ry* allele. If the observed increase in the recovery of rosy+ flies is because recombinants in which restoration to *ry*- would have occurred are instead recovered as mosaics, we predict a greater increase in NCOs than COs, since recovery requires inclusion of the point mutation in hDNA; this is indeed what we observe in *Msh6* mutants. These results, therefore, are consistent with a role for *Drosophila* MSH6 in the repair of mismatches in hDNA, and they suggest that the *ry* point mutations in our experiment are often subject to restoration repair.

NCOs from Msh6 mutants exhibit more PMS than COs: To more directly assess the role of MSH6 in hDNA repair, we examined the incidence of PMS among recombination events. Because XDH is secreted throughout the larva, we recover *ry*+//*ry*- mosaics as adults that are phenotypically rosy+. To detect PMS of the *ry* point mutations, we looked for the presence of maternally-inherited *ry*- chromosomes. As described previously (Chapter 3), we used two assays to detect these chromosomes: (1) transmission of a maternal *ry*- chromosome through the germline and (2) detection by PCR of *ry*- sequence using allele-specific primers. In

some PMS events, a *ry* point mutation is fully-converted but flanking polymorphisms are included in unrepaired hDNA. We looked for these by sequencing PCR products from flies that survive purine selection and examining chromatograms for double peaks.

We examined the COs and NCOs from *Msh6* mutants using all three assays. We detected PMS in 14 of 66 COs (21%) and 23 of 40 NCOs (58%). DNA preparations from one CO and two NCOs were insufficient for PCR analysis. This is the first report of a mutation in *Drosophila* that causes PMS in COs, but we were surprised to note that the frequency of PMS associated with COs was significantly lower than that associated with NCOs (p = 0.0003) because it suggests an unexpected difference in either MMR or hDNA formation between COs and NCOs. The association of PMS with both CO and NCO products from *Msh6* mutants, however, suggests that hDNA is indeed an important feature of meiotic recombination in *Drosophila* and that MSH6 is involved in the repair of mismatches in this hDNA.

Recombination in Msh6 mutants is characterized by discontinuous GC and hDNA tracts: The structure and arrangement of hDNA in recombination products can be used to infer the nature of recombination intermediates. Having successfully created a *Drosophila* MMR mutant in which we can recover unrepaired hDNA, we sought to examine the recombination events from this mutant to gain insight into the recombination process. We examined the extent of unrepaired hDNA and GC

tracts in the COs and NCOs from *Msh6* mutants through PCR and sequencing (Figure 4.1 and Figure 4.2).

Among the 66 COs from *Msh6* mutants, we observed four structural classes (Figure 4.1B): (I) "normal", with a single exchange point (51 COs; 77%); (II) an hDNA tract at a single point of exchange (7 COs; 10.5%); (III) an hDNA tract separated from a single point of exchange (3 COs; 5%); and (IV) multiple points of exchange, with or without hDNA (5 COs; 7.5%). Class I COs are indistinguishable from the COs we recovered from wild-type both in continuity (Chapter 3 BLANTON *et al.* 2005) and the distribution of exchange points throughout the 3.8 kb region between the *ry* mutations (data not shown). It is evident from this result that most COs do not require MSH6 hDNA repair; however, it is not clear whether this is a consequence of MSH6-independent MMR or whether hDNA is either not formed or is not detected in these COs. The remaining three types of COs from *Msh6* are distinct from COs from wild-type both in the appearance of unrepaired hDNA (classes II, III, and IV) and multiple exchange points or discontinuities (class IV).

We also observed four structural classes among 40 NCOs from *Msh6* mutants (Figure 4.2B): (I) a single, continuous GC tract (8 NCOs; 20%): (II) a single, continuous hDNA tract (4 NCOs; 10%); (III) a single GC tract interrupted by an hDNA tract (10 NCOs; 25%); and (IV) a discontinuous GC tract, with or without hDNA (18 NCOs; 45%). Class I NCOs are similar to NCOs observed from wild-type (Chapter 3, BLANTON *et al.* 2005) in that the GC tracts are continuous. Furthermore, all GC tract lengths observed from *Msh6* mutants have also been observed in NCOs

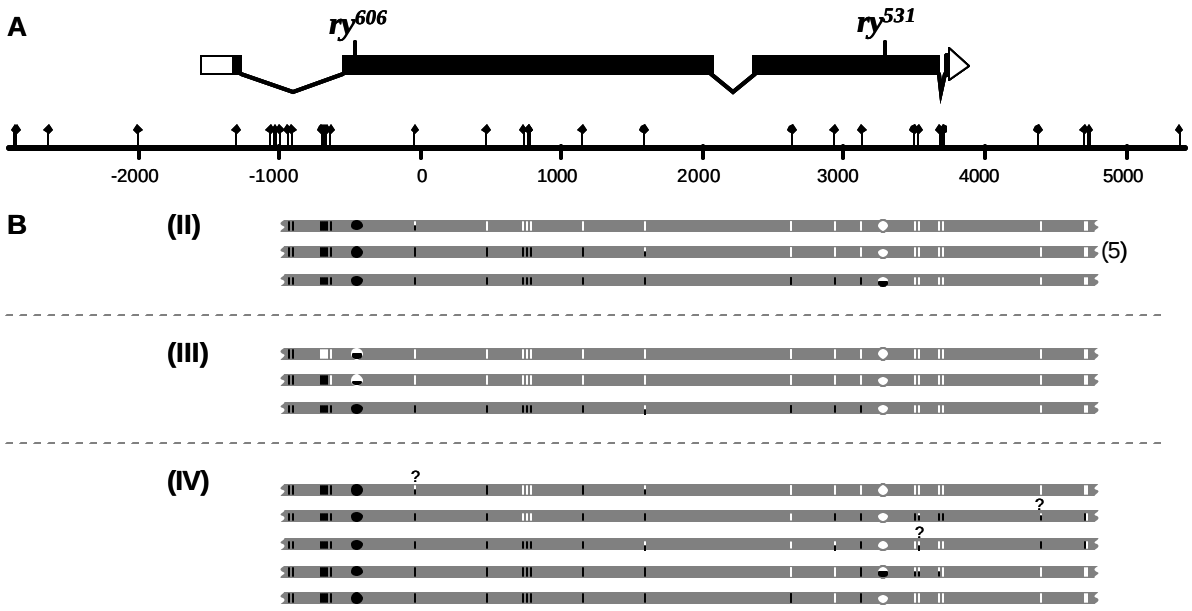

Figure 4.1. CO events from meiotic recombination in *Msh6* mutants. (A) Schematic of the *rosy* locus. Intron/exon structure is shown, with coding sequences filled. The positions of the selected sites corresponding to the ry^{606} and ry^{531} chromosomes are indicated as lollipops on the scale bar. These are all single nucleotide polymorphisms, except for -1029 and -685, which are insertions of one- and four-bp, respectively in ry^{531} relative to ry^{606}. The scale is in bp, using the coordinate system of Bender *et al*. (BENDER *et al.* 1983). (B) Markers adjacent to the exchange point in non-"normal" COs from *Msh6* mutants. Each bar represents an independent event, with the open circle denoting the selected marker (ry^{606} or ry^{531} mutant sites). Gray bars represent the region surrounding the CO event. Polymorphisms are marked with black or white lines to mark on which side of the exchange point they rest. Polymorphisms that exhibited PMS are marked with half-white, half-black lines. Black diamonds mark sites where the orientation of PMS is unknown. Events are grouped according to the numbered Classes described in the text. Class I COs are not pictured: using this scheme, they would be depicted as a simple transition from black to white at a single point.

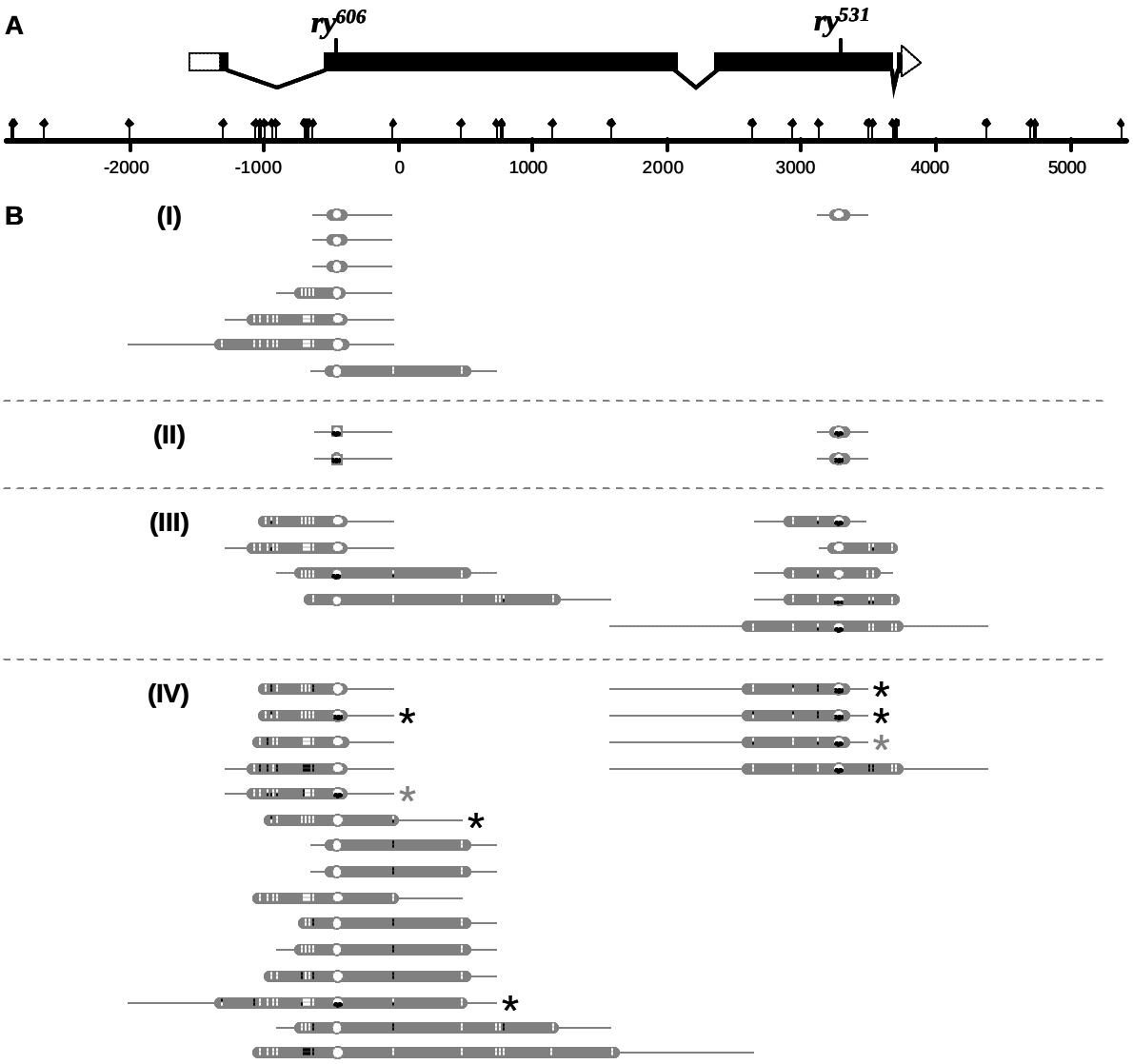

Figure 4.2. NCO events from meiotic recombination in *Msh6* mutants. (A) Schematic as in Figure 4.1. (B) Tract lengths observed in NCOs recovered from *Msh6* mutants. Gray bars represent the minimum tract length for each event, with co-converted sites marked by the white lines. Polymorphisms that were not converted (*i.e.* restored) are marked with black lines. Dotted lines represent the maximum tract length possible based on the next unconverted polymorphism. Asterisks mark events with multiple PMS patches; black asterisks mark *trans* hDNA.

from wild-type, although the small number of class I NCOs from *Msh6* mutants does not allow statistical comparison of mean GC tract lengths. The remaining three classes of NCOs from *Msh6* mutants, which represent the majority of events, are distinct from NCOs from wild-type due to the appearance of hDNA (classes II, III, and IV) and the discontinuity of tracts (classes III and IV).

Our results reveal that many recombination events from *Msh6* mutants exhibit discontinuities or "patchiness". We have identified a single discontinuous tract from wild-type (BLANTON *et al.* 2005) and two discontinuous tracts from *mei-9* mutants (Chapter 3). In each of these, a long GC tract contains a single site that appeared to undergo restoration repair. We observed many more "patchy" events from *Msh6* mutants, and these events show more complicated arrangements, sometimes including unrepaired sites or multiple discontinuities (Figure 4.1B and 4.2B), suggesting that this phenomenon is a consequence of *Msh6* mutation.

DISCUSSION

Our current understanding of the molecular mechanism of meiotic recombination is derived mostly from experimental evidence that has been collected in fungi. Although fungi have many advantages that make them amenable to studies of meiotic recombination, and these studies have greatly increased our knowledge of this process, it is important to investigate mechanisms of meiotic recombination in other organisms to determine which details are specific to a certain organism and which are universal.

One important feature of molecular models of meiotic recombination is the presence of hDNA. Investigation of hDNA in fungi has proven fruitful in many instances; however, these experiments have been limited in the structural detail they provide. We have developed a system originally designed by Chovnick and colleagues (CHOVNICK *et al.* 1970; CHOVNICK *et al.* 1971) to allow us to analyze the molecular details of recombination with high resolution in the model organism *Drosophila melanogaster* (Chapter 3, BLANTON *et al.* 2005). Unrepaired hDNA is almost never detected in wild-type *Drosophila*; therefore, we set out to increase our ability to recover hDNA using our recombination system.

In *S. cerevisiae*, the recovery of unrepaired hDNA as PMS is greatly increased in MMR-defective mutants. We created mutations in *Drosophila Msh6*, and we show that PMS is dramatically increased, suggesting that hDNA as a feature of recombination and the use of MMR to repair hDNA are both conserved in this organism. Molecular analysis of the structures of recombination events in *Msh6* mutants, however, revealed a surprising amount of discontinuity in GC and hDNA tracts.

There are several considerations to bear in mind when interpreting the impact of these results on our understanding of meiotic recombination. First, the discontinuity of events from *Msh6* mutants might reflect the structure of hDNA and GC tracts formed in recombination intermediates and products. It may be that recombination normally results in the formation of discontinuous hDNA and GC tracts, but these are masked by the action of MMR. Alternatively, loss of MMR may

cause recombination to go awry, leading to the discontinuities. Both hypotheses imply that the "patches" that we observed are not derived from hDNA, but rather were created during the recombination process, something that is not predicted by current models of meiotic recombination. It is thought that there are multiple rounds of strand invasion during repair of a double-strand gap in mitotically-dividing *Drosophila* cells (MCVEY *et al.* 2004a). Multiple rounds of invasion during meiotic recombination, in which either the homologous chromosome or sister chromatid can be used in each invasion, could lead to patchiness. Although this hypothesis could explain some of the simpler discontinuous events, it requires additional modifications to explain the complex events that we observed containing patches of conversion, restoration, and hDNA; therefore, we favor a simpler model to explain our results.

We propose that analysis of recombination events in *Msh6* mutants reveals hDNA formed during recombination, but that some of this information is lost through the action of a MSH6-independent repair pathway. We hypothesize that, because the *Drosophila* genome only encodes two MutS homologs, MSH2 and MSH6 heterodimerize to perform all canonical MMR functions; however, it remains possible that a MSH2 homodimer functions in some instances or that an as-yet-unidentified MutS ortholog exists, providing a MSH6-independent canonical MMR function in *Drosophila*. Because the MSH6-independent repair must account for the discontinuous tracts that we observed, it seems unlikely that canonical MMR proteins such as MSH2 would be responsible.

Instead, we propose that removal of the canonical MMR pathway reveals the action of an alternate or "short-patch" repair pathway in which even closely-spaced mismatches are repaired (or left unrepaired) independently. It is evident from the discontinuous events that we observed that polymorphisms as close together as 6 nucleotides can often be repaired independently (Figure 4.1B and 4.2B). The existence of this type of pathway in the absence of canonical MMR has been suggested in both *S. cerevisiae* and *Schizosaccharomyces pombe*, although the proteins involved may not be conserved between these organisms (COIC *et al.* 2000; FLECK *et al.* 1999).

If this hypothesis is true, it implies that the remaining unrepaired hDNA represents a subset of the hDNA that was formed during recombination. Examination of the PMS events, therefore, can provide insight into the meiotic recombination process. Among the PMS events in COs, we obtained ten with structures consistent with the two resolution types (Figure 4.1B, Class II and Class III) predicted by the Double-strand Break Repair (DSBR) model (SZOSTAK *et al.* 1983) (Figure 3.1). This supports the DSBR model as applicable to *Drosophila* meiotic recombination.

A prediction of the canonical DSBR model is that COs and NCOs are alternative outcomes of resolution of the same recombination intermediate; however, several lines of evidence have led to the suggestion that many NCOs are derived from synthesis-dependent strand annealing (SDSA). Both resolution and SDSA predict that within the hDNA, only one strand of the duplex may be converted,

termed *cis* hDNA (Figure 3.1). Evidence from *S. cerevisiae*, however, suggests an additional source of NCOs because some events with two tracts of hDNA in opposite orientations are observed, termed *trans* hDNA (GILBERTSON and STAHL 1996). Among the PMS events in NCOs, we often observed only a single tract of hDNA; however, in seven cases we identified two or three separate regions of hDNA (Figure 4.2B, Class IV, marked with *). In five of these, hDNA tracts were in the *trans* orientation (Figure 4.2B, Class IV, marked with black *), suggesting that, as in *S. cerevisiae*, there is a source of NCOs in addition to SDSA and resolution.

We also noted that COs are associated with PMS less frequently than NCOs in *Msh6* mutants. We have hypothesized that in *Msh6* mutants a "short-patch" repair system can act on mismatches in hDNA, reducing the level of PMS that we observe. While we cannot exclude the possibility that "short-patch" repair is more active on COs than on NCOs, a more plausible explanation is that less hDNA is present in recombination intermediates that lead to COs. According to the DSBR model, hDNA is formed either during strand invasion, during second-end capture, or during the annealing step of SDSA (Figure 3.1). Because many NCOs are proposed to arise from SDSA, a possible explanation for our results is that strand invasion and second-end capture generate less hDNA than the annealing step of SDSA. This model makes the prediction that, in *Drosophila*, GC tracts associated with COs are shorter than GC tracts associated with NCOs. Because we recover only one of the four products of meiotic recombination in our experiments, we are unable to analyze GC tracts associated with COs; however, the recovery of both chromatids involved in a

recombination event has been demonstrated in *Drosophila* (CHOVNICK *et al.* 1970), so an investigation of GC tracts associated with COs is possible.

The results reported here underscore the importance of exploiting the unique advantages of different model organisms to understand conserved processes. In particular, studying meiotic recombination in *Drosophila* provides an opportunity to investigate the length and arrangement of GC and hDNA tracts with high resolution. To this end, we created a *Drosophila* MMR mutant that allows recovery of unrepaired hDNA. We demonstrate that discontinuities in GC and hDNA tracts are common in an MMR mutant. The structure of hDNA tracts suggests that some NCOs are derived from a recombination intermediate that contains *trans* hDNA, a result that corroborates existing data in *S. cerevisiae*. Our results also suggest that associated hDNA tracts may differ in length between COs and NCOs. This supports the hypothesis that not all NCOs and COs are alternative outcomes of resolution of a common recombination intermediate.

MATERIALS AND METHODS

30 to 40 female flies *trans*-heterozygous for $Msh6^{10}$ and $Msh6^{68}$ and *trans*-heterozygous for ry^{531} and ry^{606} were crossed to 10 to 15 male flies homozygous for ry^{506}. Crosses were set up in bottles containing 25 ml of standard food medium and placed at 25°. After three days, flies were transferred to fresh media to establish a second brood, and purine was added to the first brood bottles in the amount of 0.75

ml of 0.18% (v/v) in water. One out of every twenty-five bottles was left untreated and adult progeny were counted to estimate the number of larvae screened.

Recombinant progeny were scored for flanking visible markers to determine whether a CO or GC event had occurred. The ry^{531} chromosome carried a mutation in *cv-c*, located approximately 2.1 map units distal to *ry*, and the ry^{606} chromosome carried a mutation in *kar*, located approximately 0.3 map units proximal to *ry*. Recombinants were then mated to ry^{506} flies of the opposite sex to detect mosaicism in the germline. DNA from recombinant flies was then prepared by homogenization of the entire fly in buffer containing proteinase K, as described (GLOOR *et al.* 1993), and GC tracts were determined by PCR amplification and sequencing.

To detect PMS, allele-specific PCR primers were designed to specifically amplify mutant or wild-type sequences at the two *ry* point mutations. Primers were designed such that the 3' end corresponds to the allele-specific nucleotide. A mismatch was also engineered in the primer 2 or 3 nucleotides upstream of the 3' end to increase the specificity. Each primer set was optimized for annealing temperature and magnesium concentration. In each experiment, primers were tested against control fly preps to ensure that non-specific amplification would not produce a false positive. DNA from each recombinant was tested using the corresponding wild-type and mutant allele-specific primer sets. Amplification with both allele-specific primers indicates PMS at the *ry* allele. Allele-specific PCR products were purified and sequenced to determine the length and arrangement of hDNA tracts. Extensive tracts required additional allele-specific primers for several

of the silent polymorphisms in the region. These primers were designed as described above. Additional non-allele-specific primers were used to detect PMS accompanied by full conversion of the *ry* allele. PCR products were sequenced in bulk and the chromatogram examined for double peaks.

Mean GC tract lengths and statistical comparisons were calculated as described (BLANTON *et al.* 2005). Frequency comparisons were made using Fisher's Exact Test with two-tailed *p* values, computed by Instat 3.05 (GraphPad Software).

CHAPTER 5

DISCUSSION AND FUTURE DIRECTIONS

In this thesis, I have described several experiments that have not only added to our understanding of the process of meiotic recombination, but have also brought to the forefront new questions about this process, and the tools in *Drosophila* to investigate these questions.

For the more than forty years since nicking of Holliday junctions to generate COs was first proposed, identification of an enzyme that is required for this reaction during meiotic recombination has plagued researchers. Since the cloning of *Drosophila mei-9*, we have suggested that MEI-9 might be this enzyme because of its homology to known DNA structure-specific endonucleases (SEKELSKY *et al.* 1995). The endonuclease activity of the yeast homolog of MEI-9 is dependent on interaction with a partner protein (DAVIES *et al.* 1995). In order to determine whether the proposed endonuclease function of MEI-9 in meiotic recombination similarly requires this interaction, I characterized mutants in the gene that encodes the *Drosophila* homolog, *Ercc1* (Chapter 2).

I discovered that *Ercc1* mutants are defective in meiotic recombination, suggesting that the MEI-9/ERCC1 endonuclease plays an important role in this process; however, surprisingly, the *Ercc1* defect is less severe than the *mei-9* defect

(Table 2.1 and 2.2), suggesting that MEI-9 can function independently of ERCC1. In addition to the interaction with ERCC1, MEI-9 also interacts with another protein, MUS312 (YILDIZ *et al.* 2002), and I was able to show that these interactions can be simultaneous (Figure 2.6). These results have a couple of implications. One, these results imply that the active HJ nicking enzyme may be a tripartite complex of MEI-9/ERCC1/MUS312, and two, a MEI-9/MUS312 heterodimer or a tripartite complex with a unidentified protein may also be able to act on similar structures.

One way to address these questions is through the biochemical characterization of the activity of these protein complexes. This is not a trivial undertaking. In multicellular organisms, such as *Drosophila*, meiosis typically occurs asynchronously in a small subset of cells in the gonad. Purification of the MEI-9 complex that is active during meiotic recombination directly from these cells is therefore technically challenging. Because we hypothesize that the active complex contains MEI-9, ERCC1, and MUS312, another approach is to create a system in which these three proteins can be expressed simultaneously in order to purify and assay the biochemical activity of the complex. Using a baculovirus expression system promises to be instrumental in the exploration of this question in the future.

A further implication of the hypothesis that MEI-9 nicks HJs is that in the absence of MEI-9 activity, HJ recombination intermediates must be resolved by an alternate mechanism. Many of the proposed mechanisms for the generation of both COs and NCOs differ in the structure of hDNA and GC tracts. To determine the properties of the alternate mechanism utilized in the absence of MEI-9, I took an

existing assay for the recovery of recombination events and developed it to allow the molecular characterization of hDNA and GC tracts with high resolution (Chapter 3 and BLANTON *et al.* 2005). This analysis showed that the alternate mechanism in the absence of MEI-9 generates *trans* hDNA (Figure 3.3), which we suggest is a result of dissolution of the DHJ intermediate (Figure 3.4).

This result provides further support for the hypothesis that MEI-9 nicks HJs and, again, brings the biochemical characterization of the activity of this protein to the forefront of future research. Interestingly, though, this result provides strong *in vivo* evidence for DHJ dissolution. *In vitro* evidence suggests that this process is catalyzed by the BLM helicase, a protein that is defective in a human genomic instability syndrome (WU and HICKSON 2003). Further support for DHJ dissolution as the alternate mechanism in *mei-9* mutants, therefore, might be obtained if the *trans* hDNA is dependent on the gene that encodes the *Drosophila* BLM homolog, *mus309*. In fact, *mus309* mutants alone have meiotic recombination defects (M. McVey, unpublished results); however, characterization of this defect is complicated by the sterility of *mus309* mutant females.

Although *mus309* mutant females are sterile, this sterility is not a result of a meiotic recombination defect, but rather a requirement for MUS309 in early embryogenesis (S. Andersen, unpublished results). We hypothesized that, if MUS309 is required for DHJ dissolution in the absence of MEI-9, we would observe a defect in *mei-9 mus309* double mutants prior to the embryogenesis defect. To address this question, I assessed the egg-laying ability of wild-type, *mei-9*, *mus309*,

and *mei-9 mus309* females. Results show that wild-type and *mei-9* mutants have identical egg-laying abilities (~55 eggs/female/3 days), *mus309* mutants have an intermediate defect (~30 eggs/female/3 days), and *mei-9 mus309* mutants have a severe egg-laying defect (~10 eggs/female/3 days), suggesting that there is indeed an earlier defect in the double mutants. Characterization of ovary development in *mei-9 mus309* mutants will help to determine at what stage of oogenesis the defect manifests. Additionally, we can determine whether this defect is dependent on meiotic recombination by using mutants that fail to initiate this process, such as *mei-P22* (LIU *et al.* 2002). In the future, experiments designed to bypass the sterility of *mus309* mutant females using a GAL4/UAS expression system in which *mus309* is expressed during oogenesis after the completion of meiotic recombination will allow further questions about DHJ dissolution during meiotic recombination to be addressed.

As evidenced by the results from *mei-9* mutants, molecular characterization of hDNA and GC tracts can reveal much about the pathways used to generate COs and NCOs. In fact, this has been an area of focus among yeast researchers for many years. Development of an assay that allows the molecular characterization of hDNA and GC tracts in *Drosophila* increases the tools available for investigating this process. Additionally, *Drosophila* has the distinct advantage of allowing this analysis to be carried out with much higher resolution than is possible in yeast. The full characterization of hDNA and GC tracts, however, requires the recovery of unrepaired mismatches in hDNA, a phenomenon that occurs rarely in *Drosophila*.

In order to further develop the utility of this assay, therefore, I created a *Drosophila* MMR mutant, and showed that hDNA frequently goes unrepaired in this mutant (Chapter 4). With the addition of the ability to recover hDNA at high frequency, the door is now open to the characterization of hDNA and GC tracts in *Drosophila* meiotic mutants to gain insight into their functions.

Although this mutant can be used as a tool for meiotic recombination experiments, characterization of this mutant can also lead to important insights into MMR in *Drosophila*. The genomes of most eukaryotic model organisms encode several MutS and MutL homologs. Both the *Drosophila* and *C. elegans* genomes, however, encode only a subset of these proteins, raising questions about how MMR is accomplished in these organisms. *Drosophila* presents an exciting opportunity for the study of this "pared-down" version of MMR using a model organism with many well-developed genetic tools.

Additionally, very little is known about the "short-patch" repair pathway in any organism. Evidence of "short-patch" repair has only been observed in the absence of canonical MMR (COIC *et al.* 2000), suggesting that this pathway may be prevented by the action of canonical MMR. This fits with the observation that GC and hDNA tracts in *Drosophila Msh6* mutants frequently show evidence of "short-patch" repair (Chapter 4). Also, in *Drosophila mei-9* mutants, there is some failure of repair because PMS is observed, but this never shows evidence of "short-patch" repair (Chapter 3), possibly because the canonical MMR proteins are present. Alternatively, MEI-9 may in fact be required for "short-patch" repair in *Drosophila*.

In *Schizosaccharomyces pombe*, it has been suggested that the MEI-9 homolog, Rad16p, is required for repair in the absence of canonical MMR (FLECK *et al.* 1999). If MEI-9 is indeed involved in "short-patch" repair, this predicts that analysis of meiotic recombination in a *mei-9 Msh6* mutant would reveal all hDNA formed during meiotic recombination by removing both canonical MMR and "short-patch" repair.

Analysis of hDNA and GC tracts recovered from the *Drosophila* MMR mutant has also raised many questions about the process of meiotic recombination. Among NCOs, I detected *trans* hDNA, suggesting that NCOs can be generated by multiple recombination pathways. Further experiments are necessary to explore the mechanisms involved. Additionally, results from the analysis of hDNA and GC associated with COs in the *Drosophila* MMR mutant suggest that hDNA associated with COs is shorter than hDNA associated with NCOs. One way to address this question is to use a "half-tetrad" experiment (BALDWIN and CHOVNICK 1967; CHOVNICK *et al.* 1970). By combining the assay that I have developed with the recovery of both chromatids involved in the recombination event, there is the potential for learning much about the process of meiotic recombination.

The experiments described in this thesis have led us to answers about the process of meiotic recombination, but it is clear that many more questions have also been raised. This demonstrates the exciting future potential of *Drosophila* research in this field, both in addressing existing questions and bringing forth new ideas about the crucial process of generating COs during meiosis.

REFERENCES

ADAMS, M. D., M. MCVEY and J. SEKELSKY, 2003 *Drosophila* BLM in double-strand break repair by synthesis-dependent strand annealing. Science **299:** 265-267.

ALANI, E., R. A. G. REENAN and R. D. KOLODNER, 1994 Interaction between mismatch repair and genetic recombination in *Saccharomyces cerevisiae*. Genetics **137:** 19-39.

ALLERS, T., and M. LICHTEN, 2001a Differential timing and control of noncrossover and crossover recombination during meiosis. Cell **106:** 47-57.

ALLERS, T., and M LICHTEN, 2001b Intermediates of yeast meiotic recombination contain heteroduplex DNA. Mol. Cell **8:** 225-231.

BAKER, B. S., and A. T. C. CARPENTER, 1972 Genetic analysis of sex chromosomal meiotic mutants in *Drosophila melanogaster*. Genetics **71:** 255-286.

BALDWIN, M., and A. CHOVNICK, 1967 Autosomal half-tetrad analysis in *Drosophila melanogaster*. Genetics **55:** 277-293.

BARDWELL, A. J., L. BARDWELL, A. E. TOMKINSON and E. C. FRIEDBERG, 1994 Specific cleavage of model recombination and repair intermediates by the yeast Rad1-Rad10 DNA endonuclease. Science **265:** 2082-2085.

BENDER, W., P. SPIERER and D. S. HOGNESS, 1983 Chromosomal walking and jumping to isolate DNA from the *Ace* and *rosy* loci and the bithorax complex in *Drosophila melanogaster*. J. Mol. Biol. **168:** 17-33.

BHAGAT, R., E. A. MANHEIM, D. E. SHERIZEN and K. S. MCKIM, 2004 Studies on crossover-specific mutants and the distribution of crossing over in *Drosophila* females. Cytogenet. Genome Res. **107:** 160-171.

BHUI-KAUR, A., M. F. GOODMAN and J. TOWER, 1998 DNA mismatch repair catalyzed by extracts of mitotic, postmitotic, and senescent *Drosophila* tissues and involvement of *mei-9* gene function for full activity. Mol. Cell Biol. **18:** 1436-1443.

BLANTON, H., and J. SEKELSKY, 2004 Unique invasions and resolutions: DNA repair proteins in meiotic recombination in *Drosophila melanogaster*. Cytogenet. Genome Res. **107:** 172-179.

BLANTON, H. L., S. J. RADFORD, S. MCMAHAN, H. M. KEARNEY, J. G. IBRAHIM *et al.*, 2005 REC, *Drosophila* MCM8, drives formation of meiotic crossovers. PLoS Genet. **1:** 343-353.

BORNER, G. V., N. KLECKNER and N. HUNTER, 2004 Crossover/noncrossover differentiation, synaptonemal complex formation, and regulatory surveillance at the leptotene/zygotene transition of meiosis. Cell **117:** 29-45.

BORTS, R. H., S. R. CHAMBERS and M. F. ABDULLAH, 2000 The many faces of mismatch repair in meiosis. Mutat. Res. **451:** 129-150.

BORTS, R. H., and J. E. HABER, 1987 Meiotic recombination in yeast: alteration by multiple heterozygosities. Science **237:** 1459-1465.

BOYD, J. B., M. D. GOLINO, T. D. NGUYEN and M. M. GREEN, 1976 Isolation and characterization of *X*-linked mutants of *Drosophila melanogaster* which are sensitive to mutagens. Genetics **84:** 485-506.

CARPENTER, A. T. C., 1982 Mismatch repair, gene conversion, and crossing-over in two recombination-defective mutants of *Drosophila melanogaster*. Proc. Natl. Acad. Sci. U.S.A. **79:** 5961-5965.

CARPENTER, A. T. C., 1984 Meiotic roles of crossing-over and of gene conversion. Cold Spring Harb. Symp. Quant. Biol. **49:** 23-29.

CERVANTES, M. D., J. A. FARAH and G. R. SMITH, 2000 Meiotic DNA breaks associated with recombination in *S. pombe*. Mol. Cell **5:** 883-888.

CHOVNICK, A., G. H. BALLANTYNE, D. L. BAILLIE and D. G. HOLM, 1970 Gene conversion in higher organisms: half-tetrad analysis of recombination within the *rosy* cistron of *Drosophila melanogaster*. Genetics **66:** 315-329.

CHOVNICK, A., G. H. BALLANTYNE and D. G. HOLM, 1971 Studies on gene conversion and its relationship to linked exchange in *Drosophila melanogaster*. Genetics **69:** 179-209.

COIC, E., L. GLUCK and F. FABRE, 2000 Evidence for short-patch mismatch repair in *Saccharomyces cerevisiae*. EMBO J. **19:** 3408-3417.

COLLINS, I., and C. S. NEWLON, 1994 Meiosis-specific formation of joint DNA molecules containing sequences from homologous chromosomes. Cell **76:** 65-75.

DAVIES, A. A., E. C. FRIEDBERG, A. E. TOMKINSON, R. D. WOOD and S. C. WEST, 1995 Role of the Rad1 and Rad10 proteins in nucleotide excision repair and recombination. J. Biol. Chem. **270:** 24638-24641.

DE LOS SANTOS, T., N. HUNTER, C. LEE, B. LARKIN, J. LOIDL *et al.*, 2003 The mus81/mms4 endonuclease acts independently of double-holliday junction resolution to promote a distinct subset of crossovers during meiosis in budding yeast. Genetics **164:** 81-94.

DE LOS SANTOS, T., J. LOIDL, B. LARKIN and N. M. HOLLINGSWORTH, 2001 A role for MMS4 in the processing of recombination intermediates during meiosis in *Saccharomyces cerevisiae*. Genetics **159**.

DENVER, D. R., S. FEINBERG, S. ESTES, W. K. THOMAS and M. LYNCH, 2005 Mutation rates, spectra and hotspots in mismatch repair-deficient *Caenorhabditis elegans*. Genetics **170:** 107-113.

DONALDSON, T. D., M. A. NOUREDDINE, P. J. REYNOLDS, W. BRADFORD and R. J. DURONIO, 2004 Targeted disruption of *Drosophila Roc1b* reveals functional differences in the Roc subunit of Cullin-dependent E3 ubiquitin ligases. Mol. Biol. Cell **15:** 4892-4903.

DRYSDALE, R. A., M. A. CROSBY and T. F. CONSORTIUM, 2005 Flybase: genes and gene models. Nucleic Acids Res. **33:** D390-D395.

FLECK, O., E. LEHMANN, P. SCHAR and J. KOHLI, 1999 Involvement of nucleotide-excision repair in msh2 pms1-independent mismatch repair. Nat. Genet. **21:** 314-317.

FLORES, C., and W. ENGELS, 1999 Microsatellite instability in *Drosophila spellchecker1* (MutS homolog) mutants. Proc. Natl. Acad. Sci. U.S.A. **96:** 2964-2969.

FOGEL, S., R. K. MORTIMER and K. LUSNAK, 1981, pp. 289-339 in *The Molecular Biology of the Yeast Saccharomyces*, edited by J. STRATHERN, E. W. JONES and J. BROACH. Cold Spring Harbor Laboratory, New York.

FORMOSA, T., and B. M. ALBERTS, 1986 DNA synthesis dependent on genetic recombination: Characterization of a reaction catalyzed by purified bacteriophage T4 proteins. Cell **47:** 793-806.

FOSS, H. M., K. J. HILLERS and F. W. STAHL, 1999 The conversion gradients at *HIS4* of *Saccharomyces cerevisiae*. II. A role for mismatch repair directed by biased resolution of the recombinational intermediate. Genetics **153:** 573-583.

GILBERTSON, L. A., and F. W. STAHL, 1996 A test of the double-strand break repair model for meiotic recombination in *Saccharomyces cerevisiae*. Genetics **144:** 27-41.

GLOOR, G. B., C. R. PRESTON, D. M. JOHNSON-SCHLITZ, N. A. NASSIF, R. W. PHILLIS *et al.*, 1993 Type I repressors of P element mobility. Genetics **135:** 81-95.

GUILLON, H., F. BAUDAT, C. GREY, R. M. LISKAY and B. DE MASSY, 2005 Crossover and noncrossover pathways in mouse meiosis. Mol. Cell **20:** 563-573.

HILLIKER, A. J., and A. CHOVNICK, 1981 Further observations on intragenic recombination in *Drosophila melanogaster*. Genet. Res. **38:** 281-296.

HILLIKER, A. J., S. H. CLARK and A. CHOVNICK, 1991 The effect of DNA sequence polymorphisms on intragenic recombination in the *rosy* locus of *Drosophila melanogaster*. Genetics **129:** 779-781.

HOFFMANN, E. R., and R. H. BORTS, 2005 *Trans* events associated with crossovers are revealed in the absence of mismatch repair genes in *Saccharomyces cerevisiae*. Genetics **169:** 1305-1310.

HOFFMANN, E. R., E. ERIKSSON, B. J. HERBERT and R. H. BORTS, 2005 MLH1 and MSH2 promote the symmetry of double-strand break repair events at the HIS4 hotspot in *Saccharomyces cerevisiae*. Genetics **169:** 1291-1303.

HOLLIDAY, R., 1964 A mechanism for gene conversion in fungi. Genet. Res. **78:** 282-304.

HOLLINGSWORTH, N. M., L. PONTE and C. HALSEY, 1995 *MSH5*, a novel MutS homolog, facilitates meiotic reciprocal recombination between homologs in *Saccharomyces cerevisiae* but not mismatch repair. Genes Dev. **9:** 1728-1739.

HOUTSMULLER, A. B., S. RADEMAKERS, A. L. NIGG, D. HOOGSTRATEN, J. H. HOEIJMAKERS *et al.*, 1999 Action of DNA repair endonuclease ERCC1/XPF in living cells. Science **284:** 958-961.

HUNTER, N., and R. H. BORTS, 1997 Mlh1 is unique among mismatch repair proteins in its ability to promote crossing-over during meiosis. Genes Dev. **11:** 1573-1582.

IVANOV, E. L., and J. E. HABER, 1995 *RAD1* and *RAD10*, but not other excision repair genes, are required for double-strand break-induced recombination in *Saccharomyces cerevisiae*. Mol. Cell Biol. **15:** 2245-2251.

IVANOV, E. L., N. SUGAWARA, J. FISHMAN-LOBELL and J. E. HABER, 1996 Genetic requirements for the single-strand annealing pathway for double-strand break repair in *Saccharomyces cerevisiae*. Genetics **142:** 693-704.

JAMES, P., J. HALLADAY and E. A. CRAIG, 1996 Genomic libraries and a host strain designed for highly efficient two-hybrid selection in yeast. Genetics **144:** 1425-1436.

JESSOP, L., T. ALLERS and M. LICHTEN, 2005 Infrequent co-conversion of markers flanking a meiotic recombination initiation site in *Saccharomyces cerevisiae*. Genetics **169:** 1353-1367.

JOHNSTONE, R. W., J. WANG, N. TOMMERUP, H. VISSING, T. ROBERTS *et al.*, 1998 Ciao 1 is a novel WD40 protein that interacts with the tumor suppressor protein WT1. J. Biol. Chem. **273:** 10880-10887.

JUDD, S. R., and T. D. PETES, 1988 Physical lengths of meiotic and mitotic gene conversion tracts in *Saccharomyces cerevisiae*. Genetics **118:** 401-410.

KUNKEL, T. A., and D. A. ERIE, 2005 DNA mismatch repair. Annu. Rev. Biochem. **74:** 681-710.

LIU, H., J. K. JANG, N. KATO and K. S. MCKIM, 2002 *mei-P22* encodes a chromosome-associated protein required for the initiation of meiotic recombination in *Drosophila melanogaster*. Genetics **162:** 245-258.

MCKIM, K. S., and A. HAYASHI-HAGIHARA, 1998 *mei-W68* in *Drosophila melanogaster* encodes a Spo11 homolog: evidence that the mechanism for initiating meiotic recombination is conserved. Genes Dev. **12:** 2932-2942.

MCKIM, K. S., J. K. JANG and E. A. MANHEIM, 2002 Meiotic recombination and chromosome segregation in *Drosophila* females. Annu. Rev. Genet. **36:** 205-232.

MCVEY, M., M. D. ADAMS, E. STAEVA-VIEIRA and J. SEKELSKY, 2004a Evidence for multiple cycles of strand invasion during repair of double-strand gaps in *Drosophila*. Genetics **167:** 699-705.

MCVEY, M., J. R. LAROCQUE, M. D. ADAMS and J. SEKELSKY, 2004b Formation of deletions during double-strand break repair in *Drosophila DmBlm* mutants occurs after strand invasion. Proc. Natl. Acad. Sci. U.S.A. **101:** 15694-15699.

MERKER, J. D., M. DOMINSKA and T. D. PETES, 2003 Patterns of heteroduplex formation associated with the initiation of meiotic recombination in the yeast *Saccharomyces cerevisiae*. Genetics **165:** 47-63.

MESELSON, M., and C. M. RADDING, 1975 A general model for genetic recombination. Proc. Natl. Acad. Sci. U.S.A. **72:** 358-361.

MODRICH, P., and R. LAHUE, 1996 Mismatch repair in replication fidelity, genetic recombination, and cancer biology. Annu. Rev. Biochem. **65:** 101-133.

NAG, D. K., M. A. WHITE and T. D. PETES, 1989 Palindromic sequences in heteroduplex DNA inhibit mismatch repair in yeast. Nature **340:** 318-320.

OH, J., T. BAILIN, K. FUKAI, G. H. FENG, L. HO *et al.*, 1996 Positional cloning of a gene for Hermansky-Pudlak syndrome, a disorder of cytoplasmic organelles. Nat. Genet. **14:** 300-306.

PARK, C.-H., T. BESSHO, T. MATSUNAGA and A. SANCAR, 1995 Purification and characterization of the XPF-ERCC1 complex of human DNA repair excision nuclease. J. Biol. Chem. **230:** 22657-22660.

PIRROTTA, V., 1988 Vectors for P-mediated transformation in *Drosophila*, pp. 437-456 in *Vectors. A survey of molecular cloning vectors and their uses*, edited by R. L. RODRIQUEZ and D. T. DENHARDT. Butterworths, Boston, MA.

PRAKASH, L., D. DUMAIS, R. POLAKOWSKA, G. PEROZZI and S. PRAKASH, 1985 Molecular cloning of the *RAD10* gene of *Saccharomyces cerevisiae*. Gene **34:** 55-61.

RADFORD, S. J., E. GOLEY, K. BAXTER, S. MCMAHAN and J. SEKELSKY, 2005 *Drosophila* ERCC1 is required for a subset of MEI-9-dependent meiotic crossovers. Genetics **170:** 1737-1745.

ROMANS, P., 1980a Effects of purine selection on survival of *Drosophila* mosaic for Xanthine Dehydrogenase (XDH) activity. Dros. Inf. Serv. **55:** 132-133.

ROMANS, P., 1980b Gene conversion in *mei-9*^{a}, a crossover defective mutant in *D. melanogaster*. Dros. Inf. Serv. **55:** 130-132.

RONG, Y. S., and K. G. GOLIC, 2000 Gene targeting by homologous recombination in *Drosophila*. Science **288:** 2013-2018.

RONG, Y. S., and K. G. GOLIC, 2001 A targeted gene knockout in *Drosophila*. Genetics **157:** 1307-1312.

RONG, Y. S., S. W. TITEN, H. B. XIE, M. M. GOLIC, M. BASTIANI *et al.*, 2002 Targeted mutagenesis by homologous recombination in *D. melanogaster*. Genes Dev. **16:** 1568-1581.

ROSS-MACDONALD, P., and G. S. ROEDER, 1994 Mutation of a meiosis-specific MutS homolog decreases crossing over but not mismatch correction. Cell **79:** 1069-1080.

SANDLER, L., D. L. LINDSLEY, B. NICOLETTI and G. TRIPPA, 1968 Mutants affecting meiosis in natural populations of *Drosophila melanogaster*. Genetics **60:** 525-558.

SCHIESTL, R. H., and S. PRAKASH, 1990 *RAD10*, an excision repair gene of *Saccharomyces cerevisiae*, is involved in the *RAD1* pathway of mitotic recombination. Mol. Cell Biol. **10:** 2485-2491.

SCHWACHA, A., and N. KLECKNER, 1994 Identification of joint molecules that form frequently between homologs but rarely between sister chromatids during yeast meiosis. Cell **76:** 51-63.

SCHWACHA, A., and N. KLECKNER, 1995 Identification of double Holliday junctions as intermediates in meiotic recombination. Cell **83:** 783-791.

SEKELSKY, J., M. H. BRODSKY and K. C. BURTIS, 2000a DNA Repair in *Drosophila*. Insights from the *Drosophila* genome sequence. J. Cell Biol. **150:** F31-F36.

SEKELSKY, J., K. C. BURTIS and R. S. HAWLEY, 1998 Damage control: the pleiotropy of DNA repair genes in *Drosophila melanogaster*. Genetics **148:** 1587-1598.

SEKELSKY, J., K. J. HOLLIS, A. I. EIMERL, K. C. BURTIS and R. S. HAWLEY, 2000b Nucleotide excision repair endonuclease genes in *Drosophila melanogaster*. Mutat. Res. **459:** 219-228.

SEKELSKY, J., K. S. MCKIM, G. M. CHIN and R. S. HAWLEY, 1995 The *Drosophila* meiotic recombination gene *mei-9* encodes a homologue of the yeast excision repair protein Rad1. Genetics **141:** 619-627.

STAHL, F., 1996 Meiotic recombination in yeast: coronation of the double-strand break repair model. Cell **87:** 965-968.

STURTEVANT, A. H., 1913 The linear arrangement of six sex-linked factors in *Drosophila*, as shown by their mode of association. J. Exp. Biol. **14:** 43-59.

SYMINGTON, L. S., and T. D. PETES, 1988 Expansions and contractions of the genetic map relative to the physical map of yeast chromosome III. Mol. Cell Biol. **8:** 595-604.

SZOSTAK, J. W., T. L. ORR-WEAVER, R. J. ROTHSTEIN and F. W. STAHL, 1983 The double-strand-break repair model for recombination. Cell **33:** 25-35.

TIAN, M., R. SHINKURA, N. SHINKURA and F. W. ALT, 2004 Growth retardation, early death, and DNA repair defects in mice deficient for the nucleotide excision repair enzyme XPF. Mol. Cell Biol. **24:** 1200-1205.

VILLENEUVE, A. M., and K. J. HILLERS, 2001 Whence meiosis? Cell **106:** 647-650.

WANG, T. F., N. KLECKNER and N. HUNTER, 1999 Functional specificity of MutL homologs in yeast: evidence for three Mlh1-based heterocomplexes with distinct roles during meiosis in recombination and mismatch correction. Proc. Natl. Acad. Sci. U.S.A. **96:** 13914-13919.

WEEDA, G., I. DONKER, J. DE WIT, H. MORREAU, R. JANSSENS *et al.*, 1997 Disruption of mouse *ERCC1* results in a novel repair syndrome with growth failure, nuclear abnormalities and senescence. Curr. Biol. **7:** 427-439.

WHITBY, M. C., 2005 Making crossovers during meiosis. Biochem Soc Trans **33:** 1451-1455.

WU, L., and I. D. HICKSON, 2003 The Bloom's syndrome helicase suppresses crossing over during homologous recombination. Nature **426:** 870-874.

YILDIZ, Ö., H. KEARNEY, B. C. KRAMER and J. SEKELSKY, 2004 Mutational analysis of the *Drosophila* repair and recombination gene *mei-9*. Genetics **167:** 263-273.

YILDIZ, Ö., S. MAJUMDER, B. C. KRAMER and J. SEKELSKY, 2002 *Drosophila* MUS312 interacts with the nucleotide excision repair endonuclease MEI-9 to generate meiotic crossovers. Mol. Cell **10:** 1503-1509.